J. Mech. Phys. Solids 151 (2021) 104392

Contents lists available at ScienceDirect

Journal of the Mechanics and Physics of Solids

journal homepage: www.elsevier.com/locate/jmps

Theory of fluid saturated porous media with surface effects

Xin Chen [a,b], Fei Ti [c,d], Moxiao Li [b,d,e], Shaobao Liu [c,d], Tian Jian Lu [c,d,*]

[a] Xi'an Modern Chemistry Research Institute, Xi'an 710065, PR China
[b] State Key Laboratory for Strength and Vibration of Mechanical Structures, Xi'an Jiaotong University, Xi'an 710049, PR China
[c] State Key Laboratory of Mechanics and Control of Mechanical Structures, Nanjing University of Aeronautics and Astronautics, Nanjing 210016, PR China
[d] Nanjing Center for Multifunctional Lightweight Materials and Structures (MLMS), Nanjing University of Aeronautics and Astronautics, Nanjing 210016, PR China
[e] Bioinspired Engineering and Biomechanics Center (BEBC), Xi'an Jiaotong University, Xi'an 710049, PR China

ARTICLE INFO

Keywords:
Fluid saturated porous media
Poromechanics
Surface stress
Surface effects
Biot theory

ABSTRACT

Fluid saturated porous media are abundant in nature and engineering. Existing constitutive theories of fluid saturated porous media have largely ignored surface effects, whereas recent experimental results demonstrate the importance of accounting for surface effects in constitutive modeling at micro- and nano-scales (such as brain tissue, cytoplasm, soil, oil shale, etc.), thus raising two critical issues: (1) is classical poromechanics (*e.g.*, the Biot theory) valid at sufficiently small scales, and (2) how do surface effects influence the mechanical behaviors of saturated porous media? To squarely address these issues, establishing the mechanics of solid-fluid interfaces within the porous media becomes a necessity. Built upon the homogenization assumption in the mixture theory and making use of Cauchy's theorem, we first prove mathematically that stresses on solid-fluid interfaces can be expressed by a second order tensor defined at each point of a saturated porous medium with surface effects, and then establish a rigorous theoretical framework to characterize its mechanical behaviors. Restrictions on various constitutive laws of saturated porous media developed in this framework are discussed. As an application of the developed theoretical framework, we prove that, at small deformation, the classical Biot theory still holds, at least in format, for porous media with surface effects; however, relevant parameters (*e.g.*, effective moduli) appearing in Biot's constitutive laws are dependent upon surface effects. This proof not only addresses the first issue, but also lays a solid foundation for theoretical and experimental studies of porous media with surface effects. To address the second issue, we employ the microstructures of a macromolecular network and an elastic matrix embedded with liquid inclusions as prototypes to demonstrate how their mechanical behaviors are related to the properties of three constituents (*i.e.*, solid, fluid and solid-fluid interface) and determine explicitly the parameters appearing in their constitutive relations.

1. Introduction

A fluid saturated porous medium is a kind of material in which fluid fills in the pores of its solid skeleton, and is widely found in

* Corresponding author at: State Key Laboratory of Mechanics and Control of Mechanical Structures, Nanjing University of Aeronautics and Astronautics, Nanjing 210016, PR China.
E-mail address: tjlu@nuaa.edu.cn (T.J. Lu).

https://doi.org/10.1016/j.jmps.2021.104392
Received 16 September 2020; Received in revised form 8 March 2021; Accepted 9 March 2021
Available online 12 March 2021

both nature, *e.g.*, cytoplasm, liver, skin, bone, cartilage, dentin and fruits (Cowin, 1999; Moeendarbary et al., 2013; Mow et al., 1984; Vennat et al., 2015; Wahlsten et al., 2019; Wang et al., 2020; Wei et al., 2016) and engineering, *e.g.*, oil shale, polymer, hydrogel, wood, concrete and soil (Avramidis et al., 1992; Clarkson et al., 2013; Ehlers, 2009; Kou et al., 2014; Leij et al., 2002). Ever since Darcy's classical experiments of natural sand (Darcy, 1856), the mechanical behaviors of fluid saturated porous media have been extensively investigated theoretically, numerically and experimentally, forming a discipline broadly classified as poromechanics (Coussy, 2004). Darcy used a purely experimental method to study the interaction between different components in porous media, and provided a formula (*i.e.*, Darcy's law) to describe fluid flow in porous media. To account for the deformation of solid skeleton neglected by Darcy, von Terzaghi (1923) established a set of partial differential equations governing one-dimensional consolidation in porous media, thus laying a theoretical foundation for soil mechanics. Subsequently, Biot (1941) presented a three-dimensional constitutive law for fluid-filled porous media under small deformation, and solved a series of relatively simple problems analytically. Biot and Willis (1957) discussed further how to obtain the parameters in Biot's constitutive law by experiment measurements. For analytical advantages, Rice and Cleary (1976) used stress and pore pressure as new variables to reformulate Biot's constitutive equations. In the following years, the original linear theory was generalized to finite deformations (Biot, 1977; Gajo, 2010; Nedjar, 2013), extended to cover inelastic materials (Anand, 2017; Armero, 1999) as well as solve dynamical problems (Leclaire et al., 1994; Williams, 1992). These macroscopic (phenomenological) theories are relatively straightforward, enabling solving analytically important initial-boundary value problems related to a wide range of engineering practices (Abousleiman and Cui, 1998; Cheng, 2016). However, with pore morphology and scale ignored, such theories describe porous media using a phenomenological approach: constitutive responses are either pre-defined (Nur and Byerlee, 1971) or derived from a macroscopic potential of the overall representative elementary volume (REV) (Biot and Temple, 1972; Coussy, 2004).

On the other hand, in the second half of the last century, a bottom-up approach called the mixture theory, or interactive continuum mechanics, was developed to link microscopic deformation and flow in a porous medium with its macroscopic responses. Bowen (1980) summarized key findings obtained by him (and others) with the mixture theory for incompressible and compressible porous media in the 1960′s and 1970′s. Subsequent studies of porous media mainly evolved along three directions: (1) numerical implementation of theoretical models (Schrefler et al., 1993), (2) incorporation of different material behaviors into existing models (de Boer and Ehlers, 1986a, b; de Boer and Kowalski, 1983; de Boer et al., 1991), and (3) special phenomena in saturated and empty porous solids (Baer and Nunziato, 1986).

While the purely macroscopic theories exhibit straightforwardness, mixture theories are more generic because they are derived from the system's fundamental balance laws and can account for arbitrary number of constituents that may be miscible or immiscible, chemically inert or active. Coussy et al. (1998a) and Coussy (2004) demonstrated how to derive the phenomenological Biot theory by

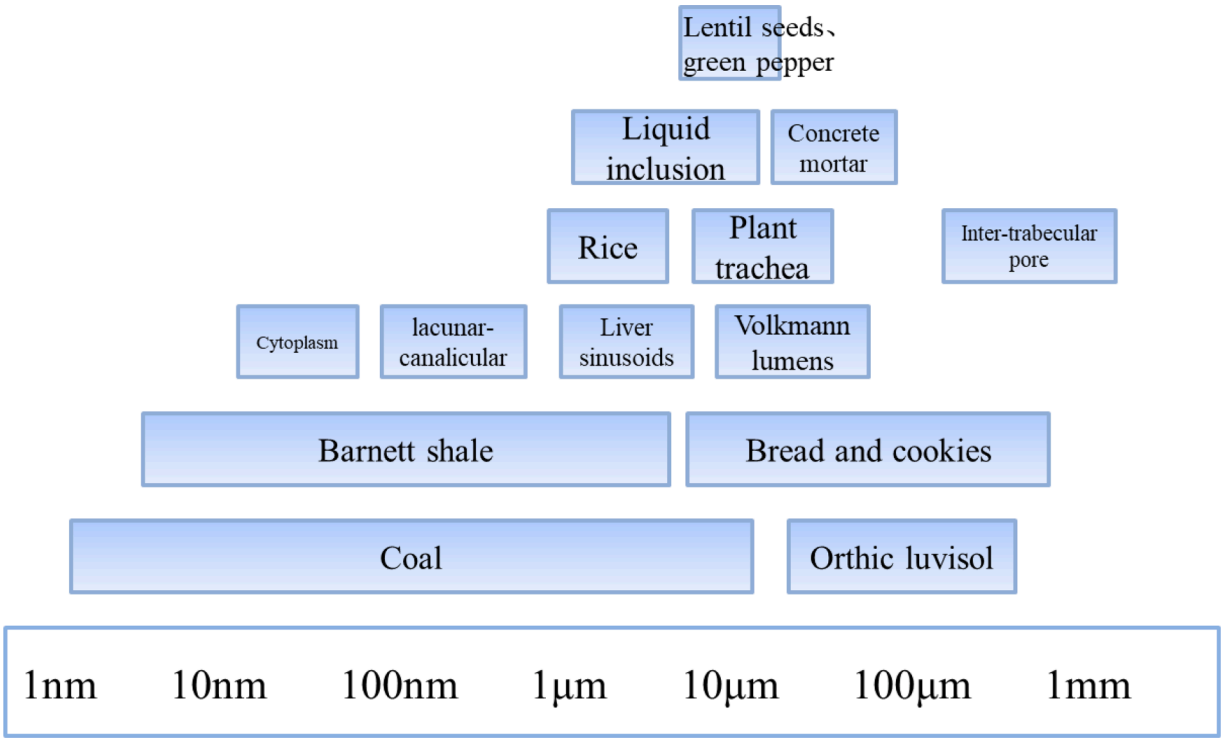

Fig. 1. Pore sizes of common fluid-filled porous media, ranging from nanometers to microns (Aouaini et al., 2015; Clarkson et al., 2013; Cowin, 1999; Hicsasmaz and Clayton, 1992; Kou et al., 2014; Le Couteur et al., 2005; Moeendarbary et al., 2013; Oikonomopoulou et al., 2011; Radlinski et al., 2004; Style et al., 2014; Vogel and Roth, 2001; Yang et al., 2010).

reformulating balance equations of the mixture theories in terms of macroscopically measurable quantities, thus showing a solid and close relationship between the two approaches. The key point of these works is that the Lagrangian Clausius–Duhem inequality of saturated porous media can be derived from the Eulerian equations of mass conservation, momentum balance (for individual components), energy conservation and entropy inequality (for the porous media). This inequality implies the existence of a single potential, which can be used for deriving constitutive relationships in terms of solid skeleton strain, fluid mass variation and temperature of the REV. By linearization, the constitutive relationships reduce to the traditional thermoporoelasticity. Such procedures provided a thermodynamic foundation for the classical Biot theory and can be used to generalize the mixture theory, *e.g.*, to consider variably saturated conditions (Coussy, 2007), phase transitions (Coussy et al., 1998b) and chemical reactions (Coussy, 2011) for porous media.

Recent developments in experimental methods enable observing and characterizing pore morphologies at increasingly small scales. Fig. 1 displays the pore sizes of common porous media, which range mainly from a few nanometers to several hundred microns. For example, the pore size in Barnett Shale varies from 5 nm to 10 μm (Clarkson et al., 2013), in cytoplasm is typically about 30 nm (Moeendarbary et al., 2013), and in liver tissue is 4–7 μm (Le Couteur et al., 2005). Nowadays, as engineering and medical practice often calls for small-scale porous media, there has been burgeoning interest in characterizing the mechanical behaviors of porous media having micro- or nano-scale pores, with significant surface effects (or size effects) identified experimentally. For typical example, surface effects in coals due to adsorption cause coal expansion or shrinkage (Cui and Bustin, 2005; Espinoza et al., 2014);

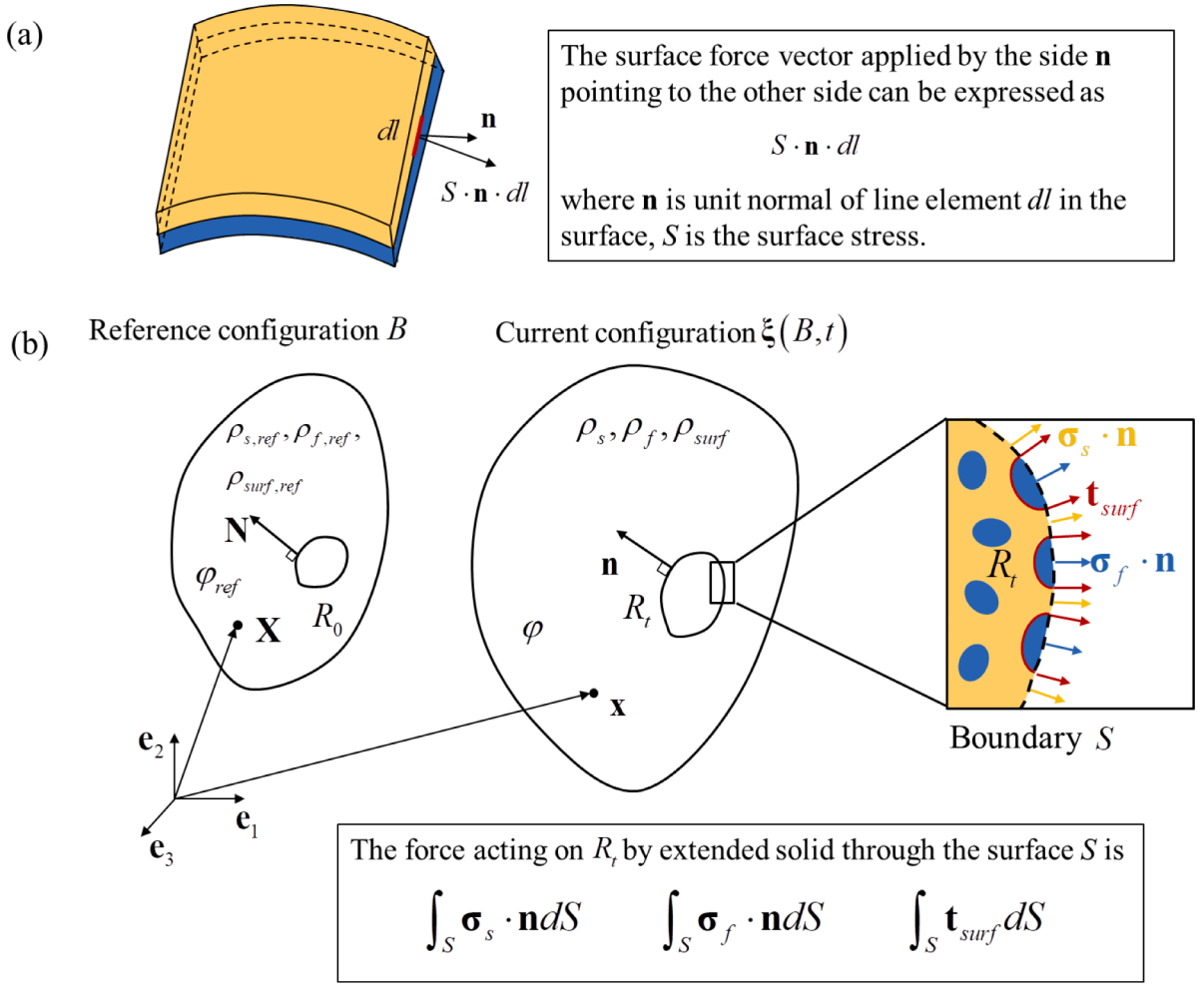

Fig. 2. Schematic of surface stress and saturated porous medium with surface effects. (a) Given a line element *dl* on a material surface, **n** is the unit normal of *dl* on the surface. The surface force vector applied by the side **n** pointing to the other side can be expressed as $\mathbf{s}\cdot\mathbf{n}dl$, where **s** is the surface stress on the material surface. (b) For a point **X** in reference configuration, **x** is its corresponding point in current configuration. φ and φ_{ref} are porous media porosity in current configuration and reference configuration, respectively. Region R_0 in reference configuration corresponds to region R_t in current configuration. **N** and **n** are outer normal vectors on the boundary of R_0 and R_t, respectively. The mass of solid skeleton and fluid in unit volume of porous medium at $\mathbf{x}=\xi(\mathbf{X},t)$ in current configuration are $\rho_s(\xi(\mathbf{X},t),t)$ and $\rho_f(\xi(\mathbf{X},t),t)$. Specific solid-fluid surface area at $\mathbf{x}=\xi(\mathbf{X},t)$ in current configuration is $\rho_{surf}(\xi(\mathbf{X},t))$. Lagrangian density at **X** in reference configuration is defined as $\rho_{a,ref}(\mathbf{X},t)=J(\mathbf{X},t)\rho_a(\xi(\mathbf{X},t),t)$, where $a=s, f$ and *surf*. Each constituent (*i.e.*, solid skeleton, fluid and solid-fluid interface) in R_t is subject to the force from the *same constituent outside the region* (arrows in different colors: orange for solid, blue for fluid, and red for solid-fluid interface).

surface effects of fluid inclusions having a size of tens of microns can significantly increase the stiffness of the elastic matrix in which these inclusions are embedded (Ducloué et al., 2014; Style et al., 2014); surface effects in hydrogels due to temperature or chemical reactions can cause large deformation, such as oscillating deformation (Dhanarajan et al., 2002; Howse et al., 2006) and volume instability (Guenther et al., 2007; Suzuki et al., 1999; Vidyasagar et al., 2008). Although these recent experimental results intuitively show significant surface effects on the mechanical behaviors of saturated porous media, these observations cause several fundamental problems. (1) Is the classical poromechanics (*e.g.*, Biot theory) valid at micro- and nano-scales? On one hand, a few modified models of porous media with surface effects have been proposed, in which the volumetric response of porous media was dependent upon the surface effects (Li and Feng, 2016). On the other hand, experiments showed that, while nano-pores in cytoplasm provide strong surface effects, the overall mechanical behaviors of cytoplasm can be still described using Biot theory without surface effects modification (Moeendarbary et al., 2013). Therefore, for saturated porous media having nano-scale pores, can we still use the Biot theory to describe their mechanical behaviors? (2) In the presence of surface effects, how the effective moduli of saturated porous media are influenced by fluids in their pores? Thus far, contradicting results were reported. On one hand, if a dry gel is immersed in aqueous environment, water will flow into the dry gel due to surface effects, forcing the gel to swell. In this case, the fluid in the pores of a porous medium softens the porous medium. On the other hand, if the fluid fills the pores of the porous medium as inclusions (*e.g.*, fluid droplets embedded in an elastic solid matrix), the presence of fluid may stiffen the porous medium due to surface effects (Ducloué et al., 2014; Style et al., 2014). To answer these fundamental questions, surface effects in saturated porous media need to be systematically investigated, especially from a theoretical perspective.

In recent years, a few theoretical studies had been carried out to characterize the surface effects of saturated porous media: for example, inclusion theories with surface effects were developed to solve the elastic fields near liquid inclusions (Style et al., 2015) and estimate the effective moduli (Mancarella et al., 2016a, 2016b). Nonetheless, these studies are limited to small deformation of close-celled porous media, *e.g.*, liquid inclusions embedded in an elastic matrix. Besides liquid inclusions, theoretical methods have been also proposed to construct constitutive relations of hydrogels (Cai and Suo, 2011; Hong et al., 2008), with simplified hydrogel microstructure (*e.g.*, a network consisting of totally random polymer chains) assumed. Note in particular that, because the Helmholtz free energy selected by these authors includes the interaction between fluid and solid skeleton, swelling and snap-though instability of the gel due to surface effects were successfully predicted, even if the classical poromechanical framework without surface effects was employed in their theoretical modeling. This is intriguing because a continuum framework should contain the contributions of all types of energy in the system from which equilibrium corresponding to each type can be derived.

Theoretical models have also been developed to characterize the adsorption deformation of porous media induced by surface effects (Vandamme et al., 2010; Zhang, 2018). These models employed a three-dimensional second-order tensor at each point in the porous medium to represent surface effects. Such treatment of surface effects is compatible with the classical poromechanics (which uses a three-dimensional second-order tensor to represent stress), but different from the treatment in surface mechanics. In fact, surface mechanics originated from Gurtin and Murdoch (1975), who established a two-dimensional tensor on material surface to describe surface stress using a strict mathematical method, as illustrated schematically in Fig. 2(a). The treatment in surface mechanics has a clear physical meaning, achieving great success in micro/nano-mechanics for, *e.g.*, nanowires (Cuenot et al., 2004; Jing et al., 2006), nano-beams (Miller and Shenoy, 2000) and nano-inhomogeneities (Duan et al., 2005a, b). Therefore, in comparison with the two-dimensional second-order tensor on material surface, whether a three-dimensional tensor at each point of a porous medium can be used to describe surface effects needs to be clarified. Further, built upon the surface mechanics as detailed above, can we establish a description method for saturated porous media with surface effects? There are two difficulties to do this. First, surface stress can only be calculated if the shape of the surface is known. However, it is difficult to accurately describe a solid-fluid surface in a saturated porous medium. Second, while equilibrium in traditional poromechanics framework is the balance in a three-dimensional space, equilibrium in surface mechanics is essentially the balance on a two-dimensional material surface. Therefore, mathematically, it is also difficult to describe surface effects in saturated porous media using the two-dimensional second-order tensor of surface mechanics.

In the current study, to answer the questions raised above, we use the mixture theory to establish a general framework for saturated porous media with surface effects. The paper is organized as follows. First of all, we will give a short description of surface mechanics in Section 2.1 and state fundamental assumptions of the mixture theory in Section 2.2. The most important assumption of the mixture theory is homogenization assumption (de Boer, 1996). With the homogenization assumption, we will convert the surface stress on a material surface into a surface traction vector acting on any appointed surface (not necessarily a material surface; Fig. 2(b)). Note that the surface traction vector is not a tensor yet but, in Section 3.3, we will prove that the surface traction vector induced by surface effects between solid skeleton and fluid can be replaced by a three-dimensional second order tensor using Cauchy's theorem. To this end, in Section 3, we start to analyze the mechanical behaviors of saturated porous media under surface effects, first with kinematics presented in 3.1. Then we state governing equations of the problem, including mass conservation in 3.2, momentum balance in 3.3, energy balance in 3.4 and the second law of thermodynamics in 3.5. In Section 4, based on constitutive assumptions for the three constituents (*i.e.*, solid, fluid and their surfaces), we discuss general restrictions on constitutive laws of porous media under surface effects. Linearization of these constitutive laws is carried out in Section 5. As an application, in Section 6, we employ the microstructures of a macromolecular network and an elastic matrix embedded with liquid inclusions as prototypes to demonstrate how their mechanical behaviors are related to the properties of three constituents (*i.e.*, solid, fluid and solid-fluid interface) and determine explicitly the parameters appearing in their constitutive relations.

2. Foundations of poromechanics with surface effects

2.1. Continuum description of surface mechanics

The continuous medium description of a material surface originates from Gurtin and Murdoch (1975), who ignored the thickness of the surface and used mathematical methods to establish a symmetrical second-order tensor in the surface to represent the surface force. Such a framework of surface mechanics is similar to that of solid mechanics: surface geometrical equations, surface constitutive equations and surface equilibrium equations together complete the description of surface mechanics problems, with surface equilibriums coupled with the equilibriums of materials on both sides of the surface. This mechanical description includes the Laplace-Young equation and the Shuttleworth equation (Shuttleworth, 1950) as special cases, and has been widely used in the development of micro-nano mechanics to account for surface effects.

We do not intend to present herein a full description of the continuum framework of surface mechanics, but rather emphasize one critical issue: surface stress is a symmetric second-order tensor $\mathbf{s}$ inside a material surface. In other words, as shown in Fig. 2(a), if a micro-line element with length dl is given in the material surface, its normal vector is $\mathbf{n}$. Then on the surface, the surface traction vector applied by the side $\mathbf{n}$ pointing to the other side can be expressed as $\mathbf{s}\cdot\mathbf{n}dl$, and this traction vector lies within the surface under consideration.

2.2. Basic assumptions of the mixture theory

At each point of the body considered, the mixture theory assumes that all constituents, which are solid, fluid and their surfaces in this study, are homogenized at the point (de Boer, 1996; Diebels and Ehlers, 1996). The point is thus a physically hypothetical concept, but it enables considering the kinetics and balance laws of each constituent at the point. Basic assumptions of the mixture theory are:

(1) All properties of the mixture must be mathematical consequences of properties of its constituents.
(2) So as to describe the motion of a constituent, we may in imagination isolate it from the rest of the mixture, provided we allow properly for the actions of the other constituents on it.
(3) The motion of the mixture is governed by the same equations as is a single body.

For a porous medium with surface effects, surface stress on solid-fluid surfaces must be considered. In the framework of mixture theory, the surface stress should be homogenized at each point of the porous medium. To do this strictly, we make the following assumption:

(1) Upon any smooth, closed orientable surface S, be it imagined surface within the porous medium or the boundary surface of the porous medium itself, there exists an integrable field of traction vector $\mathbf{t}_{surf}$ that describes the action exerted by the solid-fluid surface exterior to S on that interior to S, as shown schematically in Fig. 2(b). We further postulate that the vector field $\mathbf{t}_{surf}$ depends on time t, the spatial point $\mathbf{x}$, and the unit vector $\mathbf{n}$ of surface S, *i.e.*, $\mathbf{t}_{surf}(\mathbf{x},t,\mathbf{n})$.

In surface mechanics, surface stress is defined as a second-order tensor on material surface. The rationality of assumption (4) is that the boundary S intersects a sufficient number of solid-fluid interfaces. Therefore, the total force applied to a solid-fluid surface inside S from a solid-fluid surface outside S can be expressed by an integral of a vector function $\mathbf{t}_{surf}(\mathbf{x},t,\mathbf{n})$ on boundary S.

Physically, for fluid-saturated porous media with surface effects considered in the current study, $\mathbf{t}_{surf}(\mathbf{x},t,\mathbf{n})$ represents the traction vector per unit area exerted on a surface element oriented with normal $\mathbf{n}$ induced by solid-fluid surface effects. Note that $\mathbf{t}_{surf}(\mathbf{x},t,\mathbf{n})$ is not a tensor field yet, for it depends on the surface normal vector $\mathbf{n}$. In other words, $\mathbf{t}_{surf}(\mathbf{x},t,\mathbf{n})$ may be a complex function with respect to $\mathbf{n}$, and hence it is difficult to describe surface effects using $\mathbf{t}_{surf}(\mathbf{x},t,\mathbf{n})$. To address this deficiency, in Section 3.3, we will make use of Cauchy's theorem and employ a second order tensor field to replace $\mathbf{t}_{surf}(\mathbf{x},t,\mathbf{n})$.

3. Problem description

In this section, we adopt the mixture theory to describe fluid-saturated porous media with surface effects. There are two approaches in mixture theory: the Eularian approach and the Lagrangian approach. The Eularian approach states balance laws for each spatial point, thus convenient in describing mixture problems of different fluids. In comparison, the Lagrangian approach with respect to solid skeleton is preferred in most poromechanics studies, which describe balance laws for each material point of the skeleton (Biot, 1977; Coussy, 1989). The Lagrangian approach is also employed in the present study. After describing the kinematics in 3.1, we present governing equations of the problem in sequel: mass conservation in 3.2, momentum balance in 3.3, energy balance in 3.4, and second law of thermodynamics in 3.5.

3.1. Kinematics

Consider first the description of solid skeleton deformation. We define the reference configuration B of solid skeleton as an open set with piecewise smooth boundary in a Euclidian space R^3. Let φ_0 denote the porosity of the reference configuration B. Points in B

denoted as $\mathbf{X} = (X_1, X_2, X_3) \in B$ in a Cartesian coordinate system are called material points. In the current state at time t, the material point $\mathbf{X}$ occupies a point with coordinate $\mathbf{x} = \xi(\mathbf{X}, t)$. With φ denoting the porosity of the current configuration, the deformation gradient of the solid skeleton is defined as:

$$\mathbf{F}_s = \mathrm{Grad}\xi(\mathbf{X}, t), \tag{1}$$

where $\mathrm{Grad} = \partial/\partial\mathbf{X}$ is the gradient operator with respect to material coordinate $\mathbf{X}$. The Jacobian $J = \det\mathbf{F}_s$ links the volume element of the reference configuration to that of the current configuration, as:

$$dv = JdV = \det\mathbf{F}_s dV, \tag{2}$$

from which it follows that:

$$\rho_{s,ref} = J\rho_s, \tag{3}$$

where $\rho_{s,ref}$ and ρ_s are the density of the solid at $\mathbf{X}$ and $\mathbf{x}(\mathbf{X},t)$, respectively. Given that the deformation gradient $\mathbf{F}_s$ is not symmetric, the Green strain tensor is employed to define solid skeleton deformation, which is symmetric and defined as:

$$\mathbf{C}_s = \mathbf{F}_s^T\mathbf{F}_s. \tag{4}$$

At time t, the velocity of solid skeleton at $\mathbf{x} = \xi(\mathbf{X}, t)$is:

$$\mathbf{v}_s(\mathbf{x}, t) = \mathbf{v}_s(\xi(\mathbf{X}, t), t) = \frac{d_s}{dt}\xi(\mathbf{X}, t), \tag{5}$$

Where $d_s/dt = (\partial/\partial t)|_{\mathbf{X}}$ represents the time derivative of material point $\mathbf{X}$. The acceleration of solid skeleton at $\mathbf{x} = \xi(\mathbf{X}, t)$ and time t can thence be defined by material derivative, as:

$$\mathbf{a}_s(\mathbf{x}, t) = \mathbf{a}_s(\xi(\mathbf{X}, t), t) = \frac{d_s}{dt}\mathbf{v}_s(\xi(\mathbf{X}, t), t) = \frac{d_s^2}{dt^2}\xi(\mathbf{X}, t). \tag{6}$$

Consider a surface element dA of solid skeleton in the reference configuration and the corresponding surface element da in the current configuration. Let dA and da have $\mathbf{N}$ and $\mathbf{n}$ as their unit normal vector, respectively. According to continuum mechanics (Holzapfel, 2002), we have

$$\mathbf{n}da = J\mathbf{N}\cdot\mathbf{F}_s^{-1}dA. \tag{7}$$

In the following, we will use this expression to establish equilibriums in the reference configuration.

We focus next upon the kinematics of the fluid. Because the porous medium is taken as saturated, fluid occupies all the pores of solid skeleton in the current configuration $\xi(B, t)$. At time t, let the velocity and acceleration of the fluid occupying skeleton pores at $\mathbf{x} = \xi(\mathbf{X}, t)$ be defined as:

$$\mathbf{v}_f(\mathbf{x}, t) = \mathbf{v}_f(\xi(\mathbf{X}, t), t), \tag{8}$$

$$\mathbf{a}_f(\mathbf{x}, t) = \mathbf{a}_f(\xi(\mathbf{X}, t), t). \tag{9}$$

It is obvious that both the velocity $\mathbf{v}_a$ and acceleration $\mathbf{a}_a$ ($a = sorf$) are vector functions in the current configuration, *i.e.*, they are essentially functions of space coordinates $\mathbf{x}$ and time t. However, from the right hand side of (8) and (9), $\mathbf{v}_a$ and $\mathbf{a}_a$ can also be taken as functions of material coordinates $\mathbf{X}$ and time t, so that they can also be acted by the material gradient operator Grad. Nonetheless, no matter what independent variables are selected, the nature (vectors in the current configuration) of $\mathbf{v}_a$ and $\mathbf{a}_a$ remains unchanged.

It should be noted that, different from (6) for the solid skeleton, $\mathbf{a}_f(\mathbf{X}, t) \neq \frac{d_s}{dt}[\mathbf{v}_f(\mathbf{X}, t)]$. Actually, we have:

$$\mathbf{a}_f = \frac{\partial}{\partial t}\mathbf{v}_f + \mathbf{v}_f\mathrm{grad}\mathbf{v}_f,$$

$$\frac{d_s}{dt}\mathbf{v}_f = \frac{\partial}{\partial t}\mathbf{v}_f + \mathbf{v}_s\mathrm{grad}\mathbf{v}_f,$$

where $\frac{\partial}{\partial t}$ represents the derivative with respect to spatial coordinate $\mathbf{x}$ in the current configuration. The first expression is often used in fluid mechanics (White, 2010), and the second expression is a direct result of the chain rule $\frac{d_s(\cdot)}{dt} = \frac{\partial}{\partial t}(\cdot) + \mathbf{v}_s\mathrm{grad}(\cdot)$. Substituting the first expression into the second to eliminate $\frac{\partial}{\partial t}\mathbf{v}_f$, we get

$$\mathbf{a}_f = \frac{d_s}{dt}\mathbf{v}_f + \left(\mathbf{v}_f - \mathbf{v}_s\right)\mathrm{grad}\mathbf{v}_f, \tag{10}$$

where $\mathrm{grad} = \partial/\partial\mathbf{x}$ is the spatial gradient operator with respect to current coordinate $\mathbf{x}$. If we regard $\frac{d_s}{dt}\mathbf{v}_f$ as fluid acceleration felt by the "observer" on the solid skeleton intuitively, the meaning of expression (10) is that fluid acceleration felt by the "observer" on a fluid particle is the fluid acceleration felt by the "observer" on the solid skeleton plus the fluid velocity difference between the two

"observers".

Let $\rho_f(\xi(\mathbf{X},t),t)$ denote fluid mass in unit volume of the porous medium at point$\mathbf{x}=\xi(\mathbf{X},t)$ in current configuration, namely, the Eularian density. Since we need to describe the problem in reference configuration, we define the Lagrangian fluid density at point $\mathbf{X}$ in the reference configuration as:

$$\rho_{f,ref}(\mathbf{X},t)=J(\mathbf{X},t)\rho_f(\xi(\mathbf{X},t),t). \tag{11}$$

Intuitively, the definition means putting fluid mass in the current configuration into the reference configuration.

Next we consider the solid-fluid surface. According to our assumption, the length scale of the "point" considered in this study is much greater than the pore size. We can define the Eularian specific solid-fluid surface area $\rho_{surf}(\xi(\mathbf{X},t),t)$ to be the solid-fluid surface area in unit volume of the porous medium at point $\mathbf{x}=\xi(\mathbf{X},t)$ in the current configuration. We can thence also define the Lagrangian specific solid-fluid surface area at point $\mathbf{X}$ in the reference configuration as:

$$\rho_{surf,ref}(\mathbf{X},t)=J(\mathbf{X},t)\rho_{surf}(\xi(\mathbf{X},t),t). \tag{12}$$

We adopt in the current study the Gurtin-Murdoch surface model detailed in Section 2.1, and hence neglect the thickness and mass of a material surface. It is therefore unnecessary to define a mass density for the solid-fluid surface. In addition to this, we will state the physical laws (*i.e.*, mass conservation, momentum balance, energy balance, and the second law of thermodynamics) for an arbitrary region R_t in the current configuration. Because the solid-fluid surface is "adhered" to the solid skeleton, the solid skeleton and the solid-fluid surface have the same normal velocity at the points of ∂R_t when R_t deforms. Given the arbitrariness of R_t, the solid skeleton and solid-fluid surface have the same velocity. In other words, the velocity of the solid-fluid surface can be replaced by the solid skeleton velocity $\mathbf{v}_s$ in momentum balance (Section 3.3) and energy balance (Section 3.4). In summary, in the present study, it is unnecessary to define mass density and velocity for the solid-fluid surface.

In the remaining portion of this section, we define relevant quantities regarding deformation rate. In these expressions, *i.e.*, Eqs. (13)–(16) below, subscript *s* represents the solid skeleton and *f* represents the fluid. Spatial gradient of velocity in current configuration is defined as:

$$\Gamma_a=\mathrm{grad}\mathbf{v}_a(a=s\mathrm{or}f). \tag{13}$$

The symmetric part of Γ_a is:

$$\mathbf{D}_a=\frac{1}{2}\left(\Gamma_a+\Gamma_a^T\right)(a=s\mathrm{or}f). \tag{14}$$

The material gradient of the velocity can be written as:

$$\dot{\mathbf{F}}_a=\mathrm{Grad}\mathbf{v}_a(a=s\mathrm{or}f). \tag{15}$$

From the chain rule, we have $\dot{\mathbf{F}}_a=\Gamma_a\mathbf{F}_s$. Finally, the material derivative of the Green strain tensor of the solid skeleton is given by:

$$\dot{\mathbf{C}}_s=\frac{d_s}{dt}\mathbf{C}_s=\mathbf{F}_s^T\mathbf{D}_s\mathbf{F}_s. \tag{16}$$

3.2. Conservation of mass

For each balance law, we will firstly state its integral form for a region R_0 in reference configuration (*i.e.*, B in Fig. 2(b)), with R_0 defined as an connective open set with piecewise smooth boundary ∂R_0. It should be pointed out that while fluid can transport through the boundary ∂R_0, both the solid skeleton and the solid-fluid surface cannot transport through it. Given that the mass transportation of constituents affects balance laws, the roles played by different constituents are no longer symmetric. We will thence derive local forms of the balance laws, which are expressed via a Lagrangian approach with respect to the solid skeleton.

Given that $R_0\subset B$, mass conservation for solid can be stated as:

$$\frac{d_s}{dt}\int_{R_0}\rho_{s,ref}dV=0. \tag{17}$$

At time t, the configuration of R_0 is $R_t=\xi(R_0,t)$. The mass of fluid passing through the boundary ∂R_t can be expressed as $\int_{\partial R_t}\rho_f(\mathbf{v}_f(\mathbf{x},t)-\mathbf{v}_s(\mathbf{x},t))\cdot\mathbf{n}da$. According to (4) and (12), we can state the fluid mass conservation for R_0 as:

$$\frac{d_s}{dt}\int_{R_0}\rho_{f,ref}dV+\int_{\partial R_0}\rho_{f,ref}\left[\mathbf{F}_s^{-1}\left(\mathbf{v}_f(\xi(\mathbf{X},t),t)-\mathbf{v}_s(\xi(\mathbf{X},t),t)\right)\right]\cdot\mathbf{N}dA=0, \tag{18}$$

where the first term on the left-hand side (LHS) represents the fluid mass variation in R_0 and the second term represents the transportation of fluid mass through ∂R_0.

We can define the fluid mass flux through ∂R_0 at time t as:

$$\mathbf{M}(\mathbf{X},t)=\rho_{f,ref}\mathbf{F}_s^{-1}\cdot\left[\mathbf{v}_f(\xi(\mathbf{X},t),t)-\mathbf{v}_s(\xi(\mathbf{X},t),t)\right]. \tag{19}$$

Then we can rewrite the fluid mass conservation for region R_0 as:

$$\frac{d_s}{dt}\int_{R_0}\rho_{f,ref}dV+\int_{\partial R_0}\mathbf{M}\cdot\mathbf{N}dA=0. \tag{20}$$

With continuum description of material surface adopted, the surface has negligible thickness and hence its mass conservation can be neglected.

As in continuum mechanics, we can derive separately the local forms of mass conservation for the solid skeleton and the fluid, as:

$$\frac{d_s}{dt}\rho_{s,ref}(\mathbf{X},t)=0, \tag{21}$$

$$\frac{d_s}{dt}\rho_{f,ref}(\mathbf{X},t)+\mathrm{Div}\mathbf{M}=0. \tag{22}$$

3.3. Balance of momentum

We will state first the momentum balance laws for both the solid skeleton and fluid, which are similar to those of classical poromechanics (Coussy et al., 1998a). However, the momentum balance (force balance) on solid-fluid surface is a bit more complicated. Specifically, because surface stress is a symmetric second-order tensor defined on the surface (tensor in a two-dimensional manifold), it is difficult to include the surface stress in the three-dimensional framework of mixture theory without determining the microstructure of the porous medium.

Usually, according to assumption (2) stated in Section 2.2, the mixture theory assumes the existence of partial stresses for the solid and fluid. Under the partial stresses, either the solid or fluid is balanced. Let $\sigma_s(\xi(\mathbf{X},t),t)$ and $\sigma_f(\xi(\mathbf{X},t),t)$ be the partial Cauchy stress for the solid and the fluid, respectively. The first Piola-Kirchhoff stress can thence be defined in the reference configuration, as:

$$\mathbf{P}_a(X,t)=J\sigma_a(\xi(X,t),t)\mathbf{F}_s^{-T}, \tag{23}$$

where $a=s$ for solid skeleton and $a=f$ for fluid. The first Piola-Kirchhoff stress can be used to calculate the stress vector in current configuration as $\mathbf{P}_a\cdot\mathbf{N}=\sigma_a\cdot\mathbf{n}$, where $\mathbf{n}$ is the normal vector in current configuration and $\mathbf{N}$ is the corresponding normal vector in reference configuration. Therefore, it is convenient to use the first Piola-Kirchhoff stress in the Lagrangian description. We can also define the second Piola-Kirchhoff stress, as:

$$\mathbf{S}_a(\mathbf{X},t)=J\mathbf{F}_s^{-1}\sigma_a(\xi(\mathbf{X},t),t)\mathbf{F}_s^{-T}, \tag{24}$$

where, again, $a=s$ for solid skeleton and $a=f$ for fluid. The second Piola-Kirchhoff stress is useful in the discussion of constitutive relationships.

Before we state momentum balance for each constituent, we should define a few quantities commonly used in mixture theory. To be specific, we set $\mathbf{b}_a(\xi(\mathbf{X},t),t)$ as the external force per unit mass of constituent a at $\mathbf{x}=\xi(\mathbf{X},t)$ and set $\widehat{\mathbf{f}}_a(\xi(\mathbf{X},t),t)$ as the force per unit volume of constituent a induced by other constituents at $\mathbf{x}=\xi(\mathbf{X},t)$, where $a=s$ for solid skeleton, $a=f$ for fluid, and $a=surf$ for solid-fluid surface as illustrated in Fig. 2(b).

Given the region $R_0\subset B$, the balance of momentum for solid skeleton can be stated as

$$\frac{d_s}{dt}\int_{R_0}\rho_{s,ref}\mathbf{v}_sdV=\int_{\partial R_0}\mathbf{P}_s\cdot\mathbf{N}dA+\int_{R_0}\rho_{s,ref}\mathbf{b}_sdV+\int_{R_0}J\widehat{\mathbf{f}}_sdV, \tag{25}$$

where the left-hand side (LHS) represents the variation rate of solid momentum in R_0 and the right-hand side (RHS) represents the total force acting on solid in R_0. The first term on the RHS represents the force from solid skeleton outside R_0, the second term represents the external body force, while the third term represents the force from other constituents in R_0.

Balance of momentum for fluid in R_0 can be stated as:

$$\frac{d_s}{dt}\int_{R_0}\rho_{f,ref}\mathbf{v}_fdV+\int_{\partial R_0}\mathbf{v}_f(\mathbf{M}\cdot\mathbf{N})dA=\int_{\partial R_0}\mathbf{P}_f\cdot\mathbf{N}dA+\int_{R_0}\rho_{f,ref}\mathbf{b}_fdV+\int_{R_0}J\cdot\widehat{\mathbf{f}}_fdV, \tag{26}$$

where the first term on the LHS represents the variation rate of fluid momentum in R_0 and the second term represents the transportation of fluid momentum through boundary ∂R_0. The RHS represents the total force acting on fluid in R_0. Note that, compared with the momentum balance (25) for solid skeleton, the second term on the left side of (26) is different. The physical significance of this difference is that momentum balance is stated in reference configuration: when the porous medium deforms, while the solid cannot pass through the boundary of reference configuration, the fluid can.

Now we turn to momentum balance of a solid-fluid surface. According to assumption (4) of Section 2.2, we state balance momentum of solid-fluid surface in current configuration as:

$$\int_{\partial R_t}\mathbf{t}_{surf}(\mathbf{x},t,\mathbf{n})da+\int_{R_t}\widehat{\mathbf{f}}_{surf}dv=\mathbf{0}, \tag{27}$$

where the LHS represents the total force acting on the surface in R_t. The first term represents the force from the surface outside R_t and

the second term represents the force from other constituents in R_t. Because we neglect the mass of the surface, the two terms must be balanced with each other.

It should be emphasized that $\mathbf{t}_{surf}(\mathbf{x}, t, \mathbf{n})$ is a vector function. In solid mechanics, however, tensor rather than vector is more convenient to describe mechanical interaction in a bulk material. To obtain the tensor form of surface effects between solid skeleton and fluid, Cauchy's theorem is needed, as stated below.

Lemma. (*Cauchy's theorem*) *Let $a(\mathbf{x}, t)$ and $b(\mathbf{x}, t)$ be C^1 and $c(\mathbf{x}, t, \mathbf{n})$ be C^0 scalar functions defined for all $t \in \mathrm{R}$ (or an open interval), all $\mathbf{x} \in \xi(B, t)$, and all unit vectors $\mathbf{n}$ at $\mathbf{x}$. Assume thata, b and c satisfy the master balance law in the sense that, for any region $R_0 \in B$:*

$$\frac{\partial}{\partial t}\int_{R_t} a(\mathbf{x}, t)dv = \int_{R_t} b(\mathbf{x}, t)dv + \int_{R_t} c(\mathbf{x}, t, \mathbf{n})da, \tag{28}$$

where $R_t = \xi(R_0, t)$ and $\mathbf{n}$ is the unit outward normal to $\partial\xi(R_0, t)$. Then there exists a unique vector field $\mathbf{c}(\mathbf{x}, t)$ on $\xi(B, t)$ such that $c(\mathbf{x}, t, \mathbf{n}) = \mathbf{c}(\mathbf{x}, t) \cdot \mathbf{n}$. Proof of this Lemma can be found in Marsden and Hughes (1994).

Multiplying Eq. (27) by a vector $\mathbf{u}_0$ leads to:

$$\int_{\partial R_t} \mathbf{t}_{surf}(\mathbf{x}, t) \cdot \mathbf{u}_0 da + \int_{R_t} \widehat{\mathbf{f}}_{surf} \cdot \mathbf{u}_0 dv = 0, \forall \mathbf{u}_0. \tag{29}$$

Using the Cauchy's theorem, we infer that there exists a unique vector field $\mathbf{c}(\mathbf{x}, t)$ on $\xi(B, t)$ such that $\mathbf{t}_{surf}(\mathbf{x}, t) \cdot \mathbf{u}_0 = \mathbf{c}(\mathbf{x}, t) \cdot \mathbf{n}$, $\xi(B, t)$ being the region occupied by the whole porous medium in current configuration. Because $\mathbf{t}_{surf}(\mathbf{x}, t) \cdot \mathbf{u}_0$ is a linear function of $\mathbf{u}_0$, $\mathbf{c}(\mathbf{x}, t) \cdot \mathbf{n}$ is also such a function. Then there exists a (three-dimensional) second order tensor $\sigma_{surf}(\mathbf{x}, t)$ such that $\mathbf{c}(\mathbf{x}, t) = \sigma_{surf} \cdot \mathbf{u}_0$. Substituting $\mathbf{c}(\mathbf{x}, t) = \sigma_{surf} \cdot \mathbf{u}_0$ into (27) results in:

$$\int_{\partial R_t} \mathbf{u}_0 \cdot \sigma_{surf} \cdot \mathbf{n} da + \int_{R_t} \widehat{\mathbf{f}}_{surf} \cdot \mathbf{u}_0 dv = 0, \forall \mathbf{u}_0. \tag{30}$$

Because $\mathbf{u}_0$ is an arbitrary vector, momentum balance of the solid-fluid surface can be expressed using the second order tensor $\sigma_{surf}(\mathbf{x}, t)$ as:

$$\int_{\partial R_t} \sigma_{surf} \cdot \mathbf{n} da + \int_{R_t} \widehat{\mathbf{f}}_{surf} dv = 0. \tag{31}$$

Concerning a fluid-saturated porous medium, if we take the solid-fluid surface as the third constituent with zero mass, $\sigma_{surf}(\mathbf{x}, t)$ can be regarded as the Cauchy stress for the constituent. Therefore, analogous to the solid skeleton and fluid, the first Piola-Kirchhoff stress for the solid-fluid surface can be defined as:

$$\mathbf{P}_{surf}(\mathbf{X}, t) = J\sigma_{surf}(\xi(\mathbf{X}, t), t)\mathbf{F}_s^{-T}, \tag{32}$$

and the second Piola-Kirchhoff stress as

$$\mathbf{S}_{surf}(\mathbf{X}, t) = J\mathbf{F}_s^{-1}\sigma_{surf}(\xi(\mathbf{X}, t), t)\mathbf{F}_s^{-T}. \tag{33}$$

In Lagrangian form, momentum balance of the solid-fluid surface can thence be written as:

$$\int_{\partial R_0} \mathbf{P}_{surf} \cdot \mathbf{N} dA + \int_{R_0} J\widehat{\mathbf{f}}_{surf} dV = \mathbf{0}. \tag{34}$$

As in continuum mechanics, we can derive the local form of momentum balance for the solid skeleton as:

$$\rho_{s,ref}\mathbf{a}_s = \mathrm{Div}\mathbf{P}_s + \rho_{s,ref}\mathbf{b}_s + J\widehat{\mathbf{f}}_s. \tag{35}$$

In comparison, the local form of momentum balance for the fluid is a little different from classical continuum mechanics, as:

$$\rho_{f,ref}\frac{d_s}{dt}(\mathbf{v}_f) = \mathrm{Div}\mathbf{P}_f - (\mathrm{Div}\mathbf{v}_f) \cdot \mathbf{M} + \rho_{f,ref}\mathbf{b}_f + J\widehat{\mathbf{f}}_f, \tag{36}$$

where $\frac{d_s}{dt}(\mathbf{v}_f)$ is the fluid acceleration "observed" on the solid skeleton. By the way, it is noted that (36) is equivalent to the common form of fluid momentum balance, namely:

$$\rho_{f,ref}\mathbf{a}_f = \mathrm{Div}\mathbf{P}_f + \rho_{f,ref}\mathbf{b}_f + J\widehat{\mathbf{f}}_f. \tag{37}$$

The proof is rather direct, as we only need to expand the LHS of (36) using (11).

The local form of momentum balance for the solid-fluid surface can be written as:

$$\mathrm{Div}\mathbf{P}_{surf} + J\widehat{\mathbf{f}}_{surf} = \mathbf{0}. \tag{38}$$

Because the total momentum exchange between the solid, the fluid and solid-fluid surface is zero, we arrive at:

$$\widehat{\mathbf{f}}_s + \widehat{\mathbf{f}}_f + \widehat{\mathbf{f}}_{surf} = \mathbf{0}. \tag{39}$$

3.4. Balance of energy

3.4.1. Mechanical energy theorem

Before we state energy balance of the porous medium, we derive the mechanical energy theorem in reference configuration based on momentum balance laws detailed in Section 3.3. Multiplying (35) and (38) by $\mathbf{v}_s$, we get:

$$\rho_{s,ref}\left(\frac{d_s}{dt}\mathbf{v}_s\right)\cdot\mathbf{v}_s = \mathrm{Div}\mathbf{P}_s\cdot\mathbf{v}_s + \rho_{s,ref}\mathbf{b}_s\cdot\mathbf{v}_s + J\widehat{\mathbf{f}}_s\cdot\mathbf{v}_s, \tag{40}$$

and

$$0 = \mathrm{Div}\mathbf{P}_{surf}\cdot\mathbf{v}_s + J\widehat{\mathbf{f}}_{surf}\cdot\mathbf{v}_s. \tag{41}$$

Multiplying (36) by $\mathbf{v}_f$, we get:

$$\rho_{f,ref}\mathbf{v}_f\frac{d_s}{dt}(\mathbf{v}_f) = \mathrm{Div}(\mathbf{P}_f)\cdot\mathbf{v}_f - \mathbf{v}_f\frac{\partial\mathbf{v}_f}{\partial\mathbf{X}}\mathbf{M} + \rho_{f,ref}\mathbf{b}_f\cdot\mathbf{v}_f + J\widehat{\mathbf{f}}_f\cdot\mathbf{v}_f. \tag{42}$$

And multiplying (22) by $\frac{1}{2}\mathbf{v}_f\cdot\mathbf{v}_f$, we get:

$$\frac{1}{2}\mathbf{v}_f\cdot\mathbf{v}_f\frac{d_s}{dt}\rho_{f,ref} + \frac{1}{2}\mathbf{v}_f\cdot\mathbf{v}_f\mathrm{Div}\mathbf{M} = 0. \tag{43}$$

Upon integrating (40), (41), (42) and (43) by parts over R_0 and summing the three resulting equations, we finally obtain the mechanical energy theorem in the following form:

$$\dot{\mathscr{W}}_{ext} = \dot{\mathscr{K}}_{in} + \dot{\mathscr{W}}_d + \dot{\mathscr{K}}_{trans}, \tag{44}$$

where

$$\dot{\mathscr{K}}_{in} = \frac{d_s}{dt}\int_{R_0}\frac{1}{2}\left[\rho_{f,ref}(\mathbf{v}_f\cdot\mathbf{v}_f) + \rho_{s,ref}(\mathbf{v}_s\cdot\mathbf{v}_s)\right]dV, \tag{45}$$

$$\dot{\mathscr{W}}_d = \int_{R_0}\left(\mathbf{P}_s:\dot{\mathbf{F}}_s^T + \mathbf{P}_f:\dot{\mathbf{F}}_f^T + \mathbf{P}_{surf}:\dot{\mathbf{F}}_s^T - J\mathbf{v}_s\cdot\widehat{\mathbf{f}}_s - J\mathbf{v}_f\cdot\widehat{\mathbf{f}}_f - J\mathbf{v}_s\cdot\widehat{\mathbf{f}}_{surf}\right)dV, \tag{46}$$

$$\dot{\mathscr{W}}_{ext} = \int_{R_0}\left(\rho_{s,ref}\mathbf{b}_s\cdot\mathbf{v}_s + \rho_{f,ref}\mathbf{b}_f\cdot\mathbf{v}_f\right)dV + \int_{\partial R_0}\left(\mathbf{v}_s\cdot\mathbf{P}_s + \mathbf{v}_f\cdot\mathbf{P}_f + \mathbf{v}_s\cdot\mathbf{P}_{surf}\right)\cdot\mathbf{N}dA, \tag{47}$$

$$\dot{\mathscr{K}}_{trans} = \int_{\partial R_0}\left(\frac{1}{2}\mathbf{v}_f\cdot\mathbf{v}_f\right)\mathbf{M}\cdot\mathbf{N}dA. \tag{48}$$

To derive the mechanical energy theorem (44), we have used (21).

The physical meaning of (44) can be understood as the energy input rate $\dot{\mathscr{W}}_{ext}$ by external force for region R_0 in reference configuration is equal to the sum of kinetic energy rate $\dot{\mathscr{K}}_{in}$ in R_0, strain energy rate $\dot{\mathscr{W}}_d$ stored in R_0, and fluid kinetic energy rate $\dot{\mathscr{K}}_{trans}$ brought by fluid flow.

3.4.2. Energy balance

We set $e_s(\xi(\mathbf{X},t),t)$ and $e_f(\xi(\mathbf{X},t),t)$ to be the internal energy per unit mass of solid skeleton and fluid at $\mathbf{x} = \xi(\mathbf{X},t)$, respectively, and set $e_{surf}(\xi(\mathbf{X},t),t)$ to be the internal energy per unit area of solid-fluid surface at $\mathbf{x} = \xi(\mathbf{X},t)$. Given that $R_0 \subset B$, the internal energy rate for the solid skeleton, the fluid and the solid-fluid surface can be written as:

$$\dot{\mathscr{E}}_s = \frac{d_s}{dt}\int_{R_0}\rho_{s,ref}e_s(\xi(\mathbf{X},t),t)dV, \tag{49}$$

$$\dot{\mathscr{E}}_f = \frac{d_s}{dt}\int_{R_0}\rho_{f,ref}e_f(\xi(\mathbf{X},t),t)dV, \tag{50}$$

$$\dot{\mathscr{E}}_{surf} = \frac{d_s}{dt}\int_{R_0}\rho_{surf,ref}e_{surf}(\xi(\mathbf{X},t),t)dV. \tag{51}$$

The total internal energy rate in R_0 is simply:

$$\dot{\mathscr{E}} = \dot{\mathscr{E}}_s + \dot{\mathscr{E}}_f + \dot{\mathscr{E}}_{surf}. \tag{52}$$

Because both the solid skeleton and surface cannot go through boundary ∂R_0, the internal energy transportation rate through ∂R_0 can be written as:

$$\dot{\mathscr{E}}_{trans} = \int_{\partial R_0} e_f(\xi(\mathbf{X},t),t)\mathbf{M}\cdot\mathbf{N}dA. \tag{53}$$

The kinetic energy rate of solid and fluid in R_0 can be written as:

$$\dot{\mathscr{K}}_s = \frac{d_s}{dt}\int_{R_0}\rho_{s,ref}\frac{1}{2}\mathbf{v}_s\cdot\mathbf{v}_s dV = \int_{R_0}\rho_{s,ref}\frac{d_s}{dt}\left(\frac{1}{2}\mathbf{v}_s\cdot\mathbf{v}_s\right)dV, \tag{54}$$

$$\dot{\mathscr{K}}_f = \frac{d_s}{dt}\int_{R_0}\rho_{f,ref}\frac{1}{2}\mathbf{v}_f\cdot\mathbf{v}_f dV, \tag{55}$$

where, in deriving (54), we have used the mass conservation of solid skeleton, *i.e.*, Eq. (21). Thus the total kinetic energy rate in R_0 can be expressed as:

$$\dot{\mathscr{K}}_{in} = \dot{\mathscr{K}}_s + \dot{\mathscr{K}}_f. \tag{56}$$

Because the mass of the surface is neglected, its kinetic energy is also neglected.

Similar with (53), the kinetic energy transportation rate through ∂R_0 in unit time can be written as:

$$\dot{\mathscr{K}}_{trans} = \int_{\partial R_0}\left(\frac{1}{2}\mathbf{v}_f\cdot\mathbf{v}_f\right)\cdot\mathbf{M}\cdot\mathbf{N}dA. \tag{57}$$

The energy input rate of external force for R_0 can be expressed as:

$$\dot{\mathscr{W}}_{ext} = \int_{R_0}\left(\rho_{s,ref}\mathbf{b}_s\cdot\mathbf{v}_s + \rho_{f,ref}\mathbf{b}_f\cdot\mathbf{v}_f\right)dV + \int_{\partial R_0}\left(\mathbf{v}_s\cdot\mathbf{P}_s + \mathbf{v}_f\cdot\mathbf{P}_f + \mathbf{v}_s\cdot\mathbf{P}_{surf}\right)\cdot\mathbf{N}dA, \tag{58}$$

where the first term is induced by external body force and the second term is induced by porous medium outside R_0.

Next, we consider the energy induced by heat transfer. Let $\mathbf{q}(\mathbf{x},t)$ denote the heat flux vector in current configuration, which is also termed the Eularian heat flux in existing literature. In the present study, because energy balance is described in reference configuration, we define the Lagrangian heat flux vector $\mathbf{Q}(\mathbf{X},t)$ in reference configuration by$\mathbf{Q}\cdot\mathbf{N}dA = \mathbf{q}\cdot\mathbf{n}da$, such that heat flux through boundary ∂R_0 can be written as:

$$\dot{\mathscr{L}} = \int_{\partial R_0}\mathbf{Q}\cdot\mathbf{N}dA. \tag{59}$$

Energy balance of the porous medium can then be stated as:

$$\dot{\mathscr{E}} + \dot{\mathscr{K}}_{in} = \dot{\mathscr{W}}_{ext} - \dot{\mathscr{L}} - \dot{\mathscr{E}}_{trans} - \dot{\mathscr{K}}_{trans}, \tag{60}$$

which means that the variation rate of internal energy and kinetic energy in R_0 is equal to the sum of energy rates induced by external force, heat transfer and fluid mass transfer.

From Eqs. (44) and (60), we can derive energy balance by direct calculation, as:

$$\frac{\partial_s}{\partial t}\dot{\mathscr{E}} = \dot{\mathscr{W}}_d - \dot{\mathscr{L}} - \dot{\mathscr{E}}_{trans}. \tag{61}$$

To arrive at (61), we make use of (11), (36) and (39) to reduce the strain energy rate W_d as:

$$\begin{aligned}\dot{\mathscr{W}}_d &= \int_{R_0}\left(\mathbf{P}_s:\dot{\mathbf{F}}_s^T + \mathbf{P}_f:\dot{\mathbf{F}}_f^T + \mathbf{P}_{surf}:\dot{\mathbf{F}}_s^T - J\mathbf{v}_s\cdot\widehat{\mathbf{f}}_s - J\mathbf{v}_f\cdot\widehat{\mathbf{f}}_f - J\mathbf{v}_s\cdot\widehat{\mathbf{f}}_{surf}\right)dV\\ &= \int_{R_0}\left[\left(\mathbf{P}_s + \mathbf{P}_{surf} + \mathbf{P}_f\right):\dot{\mathbf{F}}_s^T + \mathbf{P}_f:\left(\dot{\mathbf{F}}_f^T - \dot{\mathbf{F}}_s^T\right) - J\widehat{\mathbf{f}}_f\left(\mathbf{v}_f - \mathbf{v}_s\right)\right]dV\\ &= \int_{R_0}\left\{\mathbf{P}:\dot{\mathbf{F}}_s^T + \mathrm{Div}\left[\left(\mathbf{v}_f - \mathbf{v}_s\right)\cdot\mathbf{P}_f\right] + \rho_{f,ref}\left(\mathbf{b}_f - \mathbf{a}_f\right)\left(\mathbf{v}_f - \mathbf{v}_s\right)\right\}dV,\end{aligned} \tag{62}$$

where

$$\mathbf{P} = \mathbf{P}_s + \mathbf{P}_{surf} + \mathbf{P}_f \tag{63}$$

is the total first Piola-Kirchhoff stress of the porous medium.

Finally, upon substituting (62) into (61), energy balance of the porous medium is obtained as:

$$\frac{\partial_s}{\partial t}\dot{\mathscr{E}} = \int_{R_0}\left[\mathbf{P}:\dot{\mathbf{F}}_s^T - \mathrm{Div}\left(e_f\mathbf{M}\right) + \mathrm{Div}\left[\left(\mathbf{v}_f-\mathbf{v}_s\right)\cdot\mathbf{P}_f\right] + \left(\mathbf{b}_f-\mathbf{a}_f\right)\cdot\mathbf{F}_s\cdot\mathbf{M} - \mathrm{Div}\mathbf{Q}\right]dV. \tag{64}$$

From (64), the local form of energy balance can be derived as:

$$\frac{d_s}{dt}E = \mathbf{P}:\dot{\mathbf{F}}_s^T - \mathrm{Div}\left(e_f\mathbf{M}\right) + \mathrm{Div}\left[\left(\mathbf{v}_f-\mathbf{v}_s\right)\cdot\mathbf{P}_f\right] + \left(\mathbf{b}_f-\mathbf{a}_f\right)\cdot\mathbf{F}_s\cdot\mathbf{M} - \mathrm{Div}\mathbf{Q}, \tag{65}$$

where $E(\mathbf{X},t)$ is the Lagrangian total internal energy of the porous medium:

$$E(\mathbf{X},t) = \rho_{s,ref}e_s(\xi(\mathbf{X},t),t) + \rho_{f,ref}e_f(\xi(\mathbf{X},t),t) + \rho_{surf,ref}e_{surf}(\xi(\mathbf{X},t),t). \tag{66}$$

3.5. The second law of thermodynamics

We set $s_s(\xi(\mathbf{X},t),t)$ and $s_f(\xi(\mathbf{X},t),t)$ to be the entropy per unit mass of solid skeleton and fluid at $\mathbf{x}=\xi(\mathbf{X},t)$, respectively, and set $s_{surf}(\xi(\mathbf{X},t),t)$ to be the entropy per unit area of solid-fluid surface at $\mathbf{x}=\xi(\mathbf{X},t)$. Then the Lagrangian total entropy can be define as:

$$S(\mathbf{X},t) = \rho_{s,ref}s_s(\xi(\mathbf{X},t),t) + \rho_{f,ref}s_f(\xi(\mathbf{X},t),t) + \rho_{surf,ref}s_{surf}(\xi(\mathbf{X},t),t). \tag{67}$$

Given that $R_0 \subset B$, the second law of thermodynamics for the fluid-saturated porous medium can be written as:

$$\frac{d_s}{dt}\int_{R_0}SdV + \int_{\partial R_0}s_f\mathbf{M}\cdot\mathbf{N}dS + \int_{\partial R_0}\frac{\mathbf{Q}}{T}\cdot\mathbf{N}dS \geq 0. \tag{68}$$

Its local form can be derived from (68) as:

$$\frac{d_sS}{dt} + \mathrm{Div}\left(s_f\mathbf{M}\right) + \mathrm{Div}\frac{\mathbf{Q}}{T} \geq 0. \tag{69}$$

Considering $T>0$, we multiply (69) by T and rewrite the local form of the second law as:

$$T\frac{d_sS}{dt} + T\mathrm{Div}\left(s_f\mathbf{M}\right) + \mathrm{Div}\mathbf{Q} - \frac{1}{T}\mathrm{Grad}T\cdot\mathbf{Q} \geq 0. \tag{70}$$

4. Constitutive laws and the restrictions

To further consider the mechanical behavior of a fluid-saturated porous medium, we need to make a few restrictions on the constitutive laws of each of its three constituents. In particular, since this study focuses on surface effects in the porous medium, it is necessary to ensure the generality of the surface constitutive relationship. In addition, we also consider the most common and simplest assumptions for both the solid skeleton and fluid. To facilitate the discussion of constitutive relationship, we define the Helmholtz free energy of each component as:

$$\psi_a = e_a - Ts_a, (a=s,f\mathrm{or}surf), \tag{71}$$

where the definition of e_a and s_a is presented in Sections 3.4.2 and 3.5, $\psi_s(\xi(\mathbf{X},t),t)$ and $\psi_f(\xi(\mathbf{X},t),t)$ are separately the Helmholtz free energy per unit mass of solid skeleton and fluid at $\mathbf{x}=\xi(\mathbf{X},t)$ in current configuration, and $\psi_{surf}(\xi(\mathbf{X},t),t)$ is the Helmholtz free energy per unit area of solid-fluid surface at $\mathbf{x}=\xi(\mathbf{X},t)$. By the way, we can define the Lagrangian free energy of the porous medium as:

$$\Psi(\mathbf{X},t) = \rho_{s,ref}\psi_s(\xi(\mathbf{X},t),t) + \rho_{f,ref}\psi_f(\xi(\mathbf{X},t),t) + \rho_{surf,ref}\psi_{surf}(\xi(\mathbf{X},t),t). \tag{72}$$

Restrictions on Helmholtz free energy of each component are given in Section 4.1, and those on Clausius–Duhem inequality are given in Section 4.2. Constitutive relations and discussions of surface-effects are presented in Section 4.3 and Section 6, respectively.

4.1. Constitutive laws for each constituent

4.1.1. Constitutive laws for solid-fluid surface

The continuum description of a material surface originates from the classical study of Gurtin and Murdoch (Gurtin and Murdoch, 1975). They used a mathematical method to define first a second-order tensor on the surface, *i.e.*, the surface stress, to account for surface effects of the material, and then proposed a surface constitutive model - the elastic surface model. Subsequently, Gurtin and Murdoch's surface model has been widely used and greatly developed. Nonetheless, no matter how it is developed, the surface stress is always only related to the initial shape as well as current shape of the surface, with rate effects and memory effects ignored.

In the current study of fluid-saturated porous media, we employ a more general surface constitutive model. That is, the surface stress depends only on the initial shape, current shape, and temperature of the material surface. When a specific microstructure of the porous medium is given, the initial configuration of any internal solid-fluid surface in the porous medium is also given. When the macroscopic deformation of solid skeleton $\mathbf{F}_s$, the fluid density $\rho_{f,ref}$, and the temperature T are determined, the shape of the solid-fluid surface at each point $\mathbf{x}=\xi(\mathbf{X},t)$ is determined accordingly. Therefore, we can make a general assumption, as: the Helmholtz free energy ψ_{surf} of a solid-fluid surface is a scalar function only related to solid skeleton deformation $\mathbf{F}_s$, fluid density $\rho_{f,ref}$, and temperature

T.

4.1.2. Constitutive laws for solid skeleton

With focus placed upon surface effects in a fluid-saturated porous medium, to simplify the problem, we consider the most common and simplest assumptions for solid skeleton. In poromechanics, the most commonly used constitutive law of a solid skeleton is the following thermoelastic solid skeleton.

Definition. (*thermoelastic porous media*) The solid skeleton of a porous medium is called thermoelastic solid skeleton if its Helmholtz free energy ψ_s is only a function of current deformation $\mathbf{F}_s$ of the solid skeleton, fluid density $\rho_{f,ref}$ and temperature T.

In this definition, we eliminate rate and memory effects from ψ_s. Although such requirement is strict, the thermoelastic porous medium is the most popular model for practical applications. Further, as shown in the following, the definition contains the classical Biot theory as a special case. Note also that the definition is similar to the definition of thermoelastic solid in elasticity theory (Marsden and Hughes, 1994), except that the former also accounts for the effect of fluid.

4.1.3. Constitutive laws for fluid

Again, to simplify the present problem, we use the most common and simplest fluid constitutive model in porous mechanics, assuming that the state of the fluid depends only on its pressure and temperature; thus, fluid viscosity is ignored (Bennethum et al., 2000; Coussy et al., 1998a; Coussy, 2004). It follows that the Cauchy stress of the fluid is reduced to:

$$\sigma_f = -\varphi p\mathbf{I}, \tag{73}$$

where is p the true pressure of the fluid, φ is the porosity in current configuration, and $\mathbf{I}$ is the second-order unit tensor.

For a specific microstructure of the fluid-saturated porous medium, once the macroscopic deformation $\mathbf{F}_s$ of solid skeleton, fluid density $\rho_{f,ref}$, and temperature T are determined, the pressure, temperature, internal energy and entropy of the fluid inside the porous medium are determined accordingly. Then we can assume the Helmholtz free energy ψ_f of the fluid is only related to $\mathbf{F}_s$, $\rho_{f,ref}$, and T.

To facilitate further discussions, we define the Gibbs chemical potential of the fluid as:

$$g_f = e_f + \frac{p}{\rho_{f,ture}} - Ts_f, \tag{74}$$

where

$$\rho_{f,true} = \rho_f \,/\, \varphi, \tag{75}$$

is the true density of the fluid. From Eq. (94) given later at the end of Section 4.3.2, we will find that the physical meaning of g_f is the variation of Helmholtz free energy of the overall porous medium by unit fluid mass in the porous medium. In fact, the definition (74) is the same as the definition of chemical potential for ideal fluid in classical thermodynamics, which is also the most commonly adopted form of fluid chemical potential in poromechanics (Coussy et al., 1998a; Coussy, 2004; Weinstein and Bennethum, 2006; Zhang, 2018).

Similar to classical thermodynamics, the Gibbs chemical potential satisfies:

$$dg_f = \frac{dp}{\rho_{f,true}} - s_f dT. \tag{76}$$

It follows that the common properties of the Gibbs chemical potential are:

$$\frac{\partial g_f}{\partial p} = \frac{1}{\rho_{f,true}}, \frac{\partial g_f}{\partial T} = -s_f. \tag{77}$$

Eqs. (76) and (77) will be used in subsequent discussion of constitutive laws.

4.2. The Clausius–Duhem inequality

To consider further the constitutive laws, we need a form of the second law of thermodynamics different from (68) to (70), *i.e.*, the Clausius–Duhem inequality. In continuum mechanics, this inequality proves useful in the discussion of constitutive laws. To derive the Clausius–Duhem inequality in porous media, we substitute the energy balance (66) into the entropy inequality (70) to eliminate Div$\mathbf{Q}$. Straightforward calculations then lead to

$$\begin{aligned} &-\frac{d_s E}{dt} + \mathbf{P} : \mathbf{F}_s^{-T} - \mathrm{Div}\left(e_f \mathbf{M}\right) + \mathrm{Div}\left[\left(\mathbf{v}_f - \mathbf{v}_s\right) \cdot \mathbf{P}_f\right] + T\mathrm{Div}\left(s_f \mathbf{M}\right) \\ &+T\frac{d_s S}{dt} + \left(\mathbf{b}_f - \mathbf{a}_f\right) \cdot \mathbf{F}_s \cdot \mathbf{M} - \frac{1}{T}\mathrm{Grad}T \cdot \mathbf{Q} \geq 0. \end{aligned} \tag{78}$$

For further simplication, three more steps are needed. First, in the discussion of the Clausius–Duhem inequality, it is convenient to use the second type of Piola-Kirchoff stress for its symmetry, which is defined as

$$\mathbf{S} = \mathbf{F}_s^{-1}\mathbf{P}, \tag{79}$$

where $\mathbf{P} = \mathbf{P}_s + \mathbf{P}_{surf} + \mathbf{P}_f$ is the total first Piola-Kirchoff stress of the porous media. The following property

$$\mathbf{S} : \mathbf{D}_s = \mathbf{P} : \dot{\mathbf{F}}_s^{-T}, \tag{80}$$

can be derived by direct calculation.

Second, we use the simplified form (73) of the fluid Cauchy stress and the Gibbs chemical potential (74) of the fluid to simplify the divergence related terms in (78), *i.e.*

$$\begin{aligned} &-\mathrm{Div}\left(e_f\mathbf{M}\right) + \mathrm{Div}\left[\left(\mathbf{v}_f - \mathbf{v}_s\right)\cdot\mathbf{P}_f\right] + T\mathrm{Div}\left(s_f\mathbf{M}\right) \\ &= -\mathrm{Div}\left[\left(e_f + \frac{p}{\rho_{f,true}}\right)\mathbf{M}\right] + T\mathrm{Div}\left(s_f\mathbf{M}\right) \\ &= \mathrm{Div}\left[\left(g_f + s_f T\right)\mathbf{M}\right] + T\mathrm{Div}\left(s_f\mathbf{M}\right) \\ &= -g_f\mathrm{Div}\mathbf{M} - \left(\mathrm{Grad}g_f + s_f\mathrm{Grad}T\right)\mathbf{M}. \end{aligned} \tag{81}$$

Here, the derivation of the first equality uses (73), (23) and (19), the derivation of the second equality uses (74), and the derivation of the third equality uses (77).

Third, the Lagrangian total Helmholtz free energy is often used in the discussion of Clausius–Duhem inequality. Thus, substitution of (72), (80) and (81) into (78) leads to the final form of Clausius–Duhem inequality, as:

$$\Phi_I + \Phi_{ht} + \Phi_{mt} \geq 0, \tag{82}$$

where

$$\Phi_I = -\frac{d_s\Psi}{dt} - \frac{d_sT}{dt}S + \mathbf{S} : \mathbf{D}_s - g_f\mathrm{Div}\mathbf{M}, \tag{83}$$

is the dissipation caused by deformation of the solid skeleton and solid-fluid surface as well as changes in fluid content and temperature;

$$\Phi_{ht} = -\frac{1}{T}\mathrm{Grad}T\cdot\mathbf{Q}, \tag{84}$$

is the dissipation caused by heat transfer; and

$$\Phi_{mt} = \left(\mathbf{b}_f - \mathbf{a}_f - \mathrm{grad}g_f - s_f\mathrm{grad}T\right)\cdot\mathbf{F}_s\cdot\mathbf{M}, \tag{85}$$

is the dissipation caused by mass transfer.

4.3. Conduction laws of porous media with surface effects

Due to the different physical significance of Φ_I, Φ_{ht} and Φ_{mt} as stated above, the inequality (82) can be replaced by three stronger expressions, as:

$$\Phi_I \geq 0, \Phi_{ht} \geq 0, \Phi_{mt} \geq 0. \tag{86}$$

We next discuss these expressions in sequel.

4.3.1. Conduction laws

First, consider dissipation due to heat transfer in the form of Euler dissipation φ_{ht}, defined as $\varphi_{ht}dv = \Phi_{ht}dV$ or $\varphi_{ht} = \Phi_{ht}/\mathrm{det}\mathbf{F}_s$. From (84) and $\mathrm{det}\mathbf{F}_s > 0$, it follows that:

$$\varphi_{ht} = -\mathrm{grad}T\cdot\mathbf{q} \geq 0. \tag{87}$$

If grad$T$ is taken as "force" and $\mathbf{q}/T$ as "flux". For simplicity, a linear relationship between the "force" and "flux" is usually assumed:

$$\mathbf{q} = -\mathbf{k}_{ht}\mathrm{grad}T, \tag{88}$$

where $\mathbf{k}_{ht}$ is the thermal conductivity tensor (non-negative quadratic form). This is the form of Fourier's law for heat transfer.

To represent the dissipation associated with mass transfer in a more familiar way, we substitute (77) into (85) and arrive at:

$$\Phi_{mt} = \left[\rho_{f,true}\left(\mathbf{b}_f - \mathbf{a}_f\right) - \mathrm{grad}p\right]\cdot\frac{\mathbf{F}_s\cdot\mathbf{M}}{\rho_{f,true}}. \tag{89}$$

If we consider Euler dissipation φ_{mt}, defined as $\varphi_{mt}dv = \Phi_{mt}dV$, we obtain:

$$\varphi_{mt} = \left[\rho_{f,true}\left(\mathbf{b}_f - \mathbf{a}_f\right) - \text{grad}p\right] \cdot \frac{\rho_f\left(\mathbf{v}_f - \mathbf{v}_s\right)}{\rho_{f,true}}. \tag{90}$$

Similar with the case of heat transfer, we regard $\rho_{f,true}(\mathbf{b}_f - \mathbf{a}_f) - \text{grad}p$ as "force" and $\rho_f(\mathbf{v}_f - \mathbf{v}_s)/\rho_{f,true}$ as "flux", and assume a linear relationship between the "force" and "flux", so that

$$\frac{\rho_f\left(\mathbf{v}_f - \mathbf{v}_s\right)}{\rho_{f,true}} = \mathbf{k}_{mt} \cdot \left[\rho_{f,true}\left(\mathbf{b}_f - \mathbf{a}_f\right) - \text{grad}p\right], \tag{91}$$

where $\mathbf{k}_{mt}$ is the mass conductivity tensor (non-negative quadratic form). This is the form of Darcy's law for mass transfer.

4.3.2. Equilibrium laws

The assumptions made in Section 4.1 for the solid skeleton, fluid and solid-fluid surface imply that the Helmholtz free energy Ψ of the fluid-saturated porous medium only depends on the current deformation $\mathbf{F}_s$ of solid skeleton, fluid density $\rho_{f,ref}$ and temperature T. These assumptions eliminate the rate and memory effects from the porous medium considered, which are common reasons for dissipations caused by deformation of solid skeleton and solid-fluid surface as well as changes in fluid content and temperature. Thus, we will use a stronger equation:

$$\Phi_I = -\frac{d_s\Psi}{dt} - \frac{d_sT}{dt}S + \mathbf{S} : \mathbf{D}_s - g_f\text{Div}\mathbf{M} = 0, \tag{92}$$

to replace the general inequality $\Phi_I \geq 0$. Upon using methods similar to classical continuum mechanics (Marsden and Hughes, 1994), we arrive at:

$$\mathbf{S} = \frac{\partial\Psi}{\partial\mathbf{C}_s}, g_f = \frac{\partial\Psi}{\partial\rho_{f,ref}}, S = -\frac{\partial\Psi}{\partial T}, \tag{93}$$

which are analogous to the well-known literature results about thermoelastic solid (Marsden and Hughes, 1994). Eq. (93) allows us to consider the free energy Ψ as a macro potential, because it is a function of the set of macro state variables $(\mathbf{C}_s, \rho_{f,ref}, T)$ according to Section 4.1, while their conjugate variables $(\mathbf{S}, g_f, S)$ can be derived by taking partial derivatives with respect to them.

With the configuration of initial state selected as reference configuration, it is assumed that the mass of fluid in a unit volume of porous medium is $\rho_{f,0}$ in the initial state. The Lagrangian fluid mass change $m = \rho_{f,ref} - \rho_{f,0}$ is often selected in existing studies of porous media. Since $\rho_{f,0}$ is a constant, we can use $(\mathbf{C}_s, m, T)$ as equivalent independent variables in the Lagrangian free energy to replace $(\mathbf{C}_s, \rho_{f,ref}, T)$. Thence, the constitutive relationships of (93) become:

$$\mathbf{S} = \frac{\partial\Psi}{\partial\mathbf{C}_s}, g_f = \frac{\partial\Psi}{\partial m}, S = -\frac{\partial\Psi}{\partial T}. \tag{94}$$

In the remaining part of this study, we will use $(\mathbf{C}_s, m, T)$ as independent variables.

We observe that, in format, the constitutive relationships of (94) are the same as those obtained in existing literature about porous media without surface effects (Coussy et al., 1998a). In other words, the constitutive laws of classical poromechanics can be used to describe the mechanical behaviors of porous media with surface effects, as long as the contributions of surface effects to the Lagrangian free energy Ψ are considered. Physically, the underlying mechanism is rather intuitive: when a saturated porous medium deforms, the solid-fluid interface is adhered to the solid skeleton; thus, if the solid-fluid interface together with the solid skeleton are taken as a special type of solid, the classical framework of poromechanics can still be used to deal with porous media with surface effects.

5. Linearized porous media

In addition to describing mathematically the surface effects of porous media as detailed in the previous sections, in the current section, we aim to quantify such effects. For illustration, we consider the effective moduli of a fluid saturated porous medium since they are the most commonly used quantities that characterize the mechanical behaviors of a material. Generally speaking, the moduli are scale factors of stress and deformation and hence should be discussed under small deformation. Therefore, upon linearizing the constitutive relations of (94), we define the coefficients appearing in the linearized constitutive relationships as the effective moduli and then discuss their physical significance.

In accordance with the theory of linear elasticity, the second Piola-Kirchhoff stress tensor $\mathbf{S}$ is replaced by the Cauchy stress tensor σ and the Green-Lagrange strain tensor $\mathbf{C}_s$ is replaced by the linearized strain tensor ε of the solid skeleton, with ε depending upon the solid skeleton displacement vector $\mathbf{u}$ by:

$$\varepsilon_{ij} = \frac{1}{2}\left(\frac{\partial u_i}{\partial x_j} + \frac{\partial u_j}{\partial x_i}\right). \tag{95}$$

It follows then that the constitutive relationships of (94) can be expressed as:

$$\Psi = \Psi\left(\varepsilon_{ij}, m, T\right), \sigma_{ij} = \frac{\partial \Psi}{\partial \varepsilon_{ij}}, g_f = \frac{\partial \Psi}{\partial m}, S = -\frac{\partial \Psi}{\partial T}. \tag{96}$$

We linearize (96) to arrive at

$$d\sigma_{ij} = \frac{\partial^2 \Psi}{\partial \varepsilon_{ij} \partial \varepsilon_{ij}} d\varepsilon_{kl} + \frac{\partial^2 \Psi}{\partial \varepsilon_{ij} \partial m} dm + \frac{\partial^2 \Psi}{\partial \varepsilon_{ij} \partial T} dT, \tag{97}$$

$$dg_f = \frac{\partial^2 \Psi}{\partial \varepsilon_{ij} \partial m} d\varepsilon_{ij} + \frac{\partial^2 \Psi}{\partial^2 m} dm + \frac{\partial^2 \Psi}{\partial m \partial T} dT, \tag{98}$$

$$dS = -\frac{\partial^2 \Psi}{\partial T \partial \varepsilon_{ij}} d\varepsilon_{ij} - \frac{\partial^2 \Psi}{\partial m \partial T} dm - \frac{\partial^2 \Psi}{\partial^2 T} dT. \tag{99}$$

In linear elasticity, the second order derivatives of energy functional are usually taken as mechanical properties, measurable by experiments. Thus, we assume that:

$$\begin{aligned} &\frac{\partial^2 \Psi}{\partial \varepsilon_{ij} \partial \varepsilon_{kl}} = C_{ijkl}, \left(\rho_{f,true}\right)^2 \frac{\partial^2 \Psi}{\partial m^2} = M, -\frac{\partial^2 \Psi}{\partial T^2} = \frac{C_\varepsilon}{T}, \\ &\rho_{f,true} \frac{\partial^2 \Psi}{\partial \varepsilon_{ij} \partial m} = -MB_{ij}, \rho_{f,true} \frac{\partial^2 \Psi}{\partial m \partial T} = 3M\beta, -\frac{\partial^2 \Psi}{\partial T \partial \varepsilon_{ij}} = A_{ij}. \end{aligned} \tag{100}$$

Using these coefficients, we rewrite (97) to (99) as:

$$d\sigma_{ij} = C_{ijkl} d\varepsilon_{kl} - MB_{ij} \frac{dm}{\rho_{f,true}} - A_{ij} dT, \tag{101}$$

$$dg_f = \frac{M}{\rho_{f,true}} \left(- B_{ij} d\varepsilon_{ij} + \frac{dm}{\rho_{f,true}} + 3\beta dT \right), \tag{102}$$

$$dS = A_{ij} d\varepsilon_{ij} - 3M\beta \frac{dm}{\rho_{f,true}} + \frac{C_\varepsilon}{T} dT, \tag{103}$$

which similar to the classical Biot theory (Biot, 1941; Rice and Cleary, 1976). To facilitate subsequent comparison, we use the assumptions commonly adopted in the Biot theory and rewrite the above formula using the same variables introduced by Biot.

The first assumption of the Biot theory is the isotropy of porous media. So the fourth-order tensor can be represented by two scalars, as:

$$C_{ijkl} = \left(K_u - \frac{2}{3} G \right) \delta_{ij} \delta_{kl} + 2G \delta_{ik} \delta_{jl}, \tag{104}$$

where K_u is called the undrained bulk modulus of the porous medium, and G is the shear modulus of the porous media. According to (96) and (99), we get:

$$\frac{\partial g_f}{\partial \varepsilon_{ij}} = -\frac{MB_{ij}}{\rho_{f,true}}. \tag{105}$$

When the fluid-saturated porous medium is subjected to pure shear, its volume does not change. Therefore, pure shear will not cause the pressure and temperature of the fluid in the porous medium to change and hence the off-diagonal elements of the above expression are zero. In addition, considering the assumption of isotropy, we obtain a diagonal matrix, yielding:

$$B_{ij} = \alpha \delta_{ij}. \tag{106}$$

The second assumption commonly used in the Biot theory is to ignore the effect of temperature. According to (99), we can ignore the change of entropy such that we can delete (103) from the constitutive relation. In addition, the change in Gibbs chemical potential is proportional to the change in pressure, namely:

$$dg_f = \frac{dp}{\rho^f}. \tag{107}$$

In addition, Biot theory uses the fluid volume change per unit volume of porous medium to describe the state of the fluid, which is related to the mass change of the fluid per unit volume of porous medium as:

$$\zeta = \frac{m}{\rho_{f,true}}. \tag{108}$$

We assume further that the porous medium has no initial stress and initial fluid pressure. Finally, for a fluid-saturated porous

medium with surface effects under small deformation, we substitute (104)-(108) into (101)-(103) to arrive at its constitutive law, as:

$$\sigma_{ij} = \left(K_u - \frac{2}{3}G\right)\varepsilon_{kk}\delta_{ij} + 2G\varepsilon_{ij} - M\alpha\zeta\delta_{ij},$$
$$p = M(-\alpha\varepsilon_{ii} + \zeta). \tag{109}$$

which has the same form as that of the Biot theory (Biot, 1941; Rice and Cleary, 1976). In other words, under small deformation, we have proved that the constitutive relationship of a porous medium with surface effects accounted for has the same form as the classical Biot formula. Coincidentally, it has been demonstrated experimentally that, although cytoplasm exhibits complex microstructure and contains nano-pores, its mechanical behavior can be described using the Biot theory (Moeendarbary et al., 2013). Nonetheless, it should be noted that when the scale considered is too small to guarantee the rationality of continuum modeling, the assumptions stated in Section 2.2 are not satisfied. That is, at sufficiently small scales, the Biot theory may no longer be valid. But a further investigation of this extends beyond the scope of the current study.

It should be emphasized that, according to Eq. (100), the coefficients appearing in Eq. (109) are second order derivatives of the Lagrangian free energy Ψ. For a saturated porous medium, the Lagrangian free energy Ψ as defined in Eq. (72) contains surface effects. Therefore, although the constitutive relationship of a porous medium with surface effects accounted for has the same form as the classical Biot formula, the coefficients (*e.g.*, effective moduli) in the constitutive relationship are influenced by surface effects. To quantify the influence of surface effects on macroscopic mechanical responses, these coefficients need to be determined by considering specific microstructure of the porous medium.

6. Estimation of mechanical properties of porous media with surface effects under small deformation

In Section 5, we have demonstrated that the constitutive relationships of a porous medium with surface effects are given by Eq. (96), which simplify to Eq. (109) under small deformation. It should be noted that the coefficients, *i.e.*, the mechanical properties, in Eq. (109) depend on the surface effects, although the form of Eq. (109) is the same as the Biot fomula (Biot, 1941). To obtain these coefficients with surface effects considered, so that our model can be implemented for practical applications, two methods may be employed: (1) experimental determination, as demonstrated by Biot and Willis (1957); (2) theoretical estimation if the microstructure of the porous medium is known a priori. Here, we have adopted the second method for two typical microstructures, *i.e.*, macromolecular network and liquid inclusions.

It is convenient to estimate the mechanical properties of a fluid-saturated porous medium with clear physical meanings. Consid-

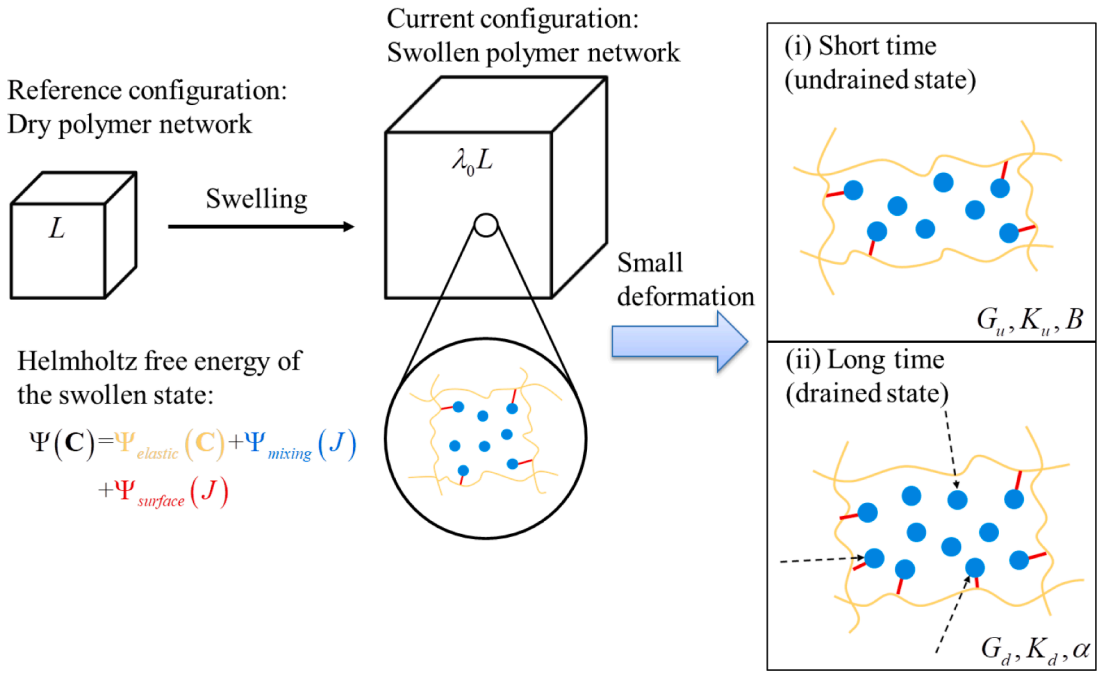

Fig. 3. Schematic of a macromolecular network filled by fluid. The solid skeleton of a typical macromolecular network is a polymer network containing cross-linked polymer chains, which are assumed to be incompressible. There exist two limit cases, *i.e.*, the short-time deformation (undrained state) and the long-time deformation (drained state). The short-time deformation locally rearranges the small molecules, so that the network can change shape but not volume. The long-time deformation (drained state) does not conserve the number of small molecules locally, so that the network can change both shape and volume.

ering there are several equivalent forms for Biot's fomula (Rice and Cleary, 1976), here we choose another class of mechanical properties with clear physical meanings to express the constitutive laws, which are the bulk modulus K_u of the undrained state (*i.e.*, the case that the fluid does not have enough time to escape from the pores), the bulk modulus K_d of the drained state (*i.e.*, the case that the fluid has enough time to escape from the pores and the fluid pressure is equal to its initial value), the shear modulus G, and the Biot effective stress coefficient α, *i.e.*, the ratio of the fluid volume gained (or lost) in a material element to the volume change of that element in the drained state. Because $M = \frac{K_u - K_d}{\alpha^2}$ (Detournay and Cheng, 1993), the constitutive equations of (109) can be rewritten using these four parameters, as:

$$\begin{aligned} \sigma_{ij} &= \left(K_u - \frac{2}{3}G\right)\varepsilon_{ij}\delta_{ij} + 2G\varepsilon_{ij} - \frac{K_u - K_d}{\alpha}\delta_{ij}\zeta, \\ p &= \frac{K_u - K_d}{\alpha}\left(-\alpha\varepsilon_{ij} + \zeta\right), \end{aligned} \tag{110}$$

where ζ represents the fluid volume change per unit volume in the porous medium.

6.1. Macromolecular network

With reference to Fig. 3, the solid skeleton of a typical macromolecular network is a polymer network containing cross-linked polymer chains, which are assumed to be incompressible. We set the reference configuration of the polymer network as the so-called dry state, in which each polymer chain is arranged randomly and no pores exist between polymer chains. If the dry polymer network is put into a solvent environment, the fluid, which is also assumed to be incompressible, will flow into the network, which stretches the network and makes the network swell. We set the swollen state of the polymer network as the current configuration. Let λ_0 be the free-swelling stretch. The external load is applied on the current configuration. If the swollen network sustains a small deformation, then according to the results of Section 5, its mechanical behaviors can be described using a constitutive law of the Biot form, *i.e.*, Eq. (110). Next, we illustrate how to connect the coefficients in Eq. (110) by properties of the solid skeleton, the fluid, and the solid-fluid surface.

According to the properties of the classical Biot model (Detournay and Cheng, 1993; Hong et al., 2009), there exist two limit cases, *i.e.*, the short-time deformation (undrained state) and the long-time deformation (drained state). The short-time deformation locally rearranges the small molecules, so that the network can change shape but not volume. The long-time deformation (drained state) does not conserve the number of small molecules locally, so that the network can change both shape and volume.

We first consider the undrained state to determine the undrained bulk modulus K_u and the Biot effective stress coefficient α. Assuming that the network and fluid are both incompressible, we can obtain the mechanical parameters in the undrained state, *i.e.*, the undrained bulk modulus as:

$$K_u = \infty, \tag{111}$$

and the Biot effective stress coefficient as:

$$\alpha = 1. \tag{112}$$

In the drained state, the mechanical behaviors of the swollen network can be described by its Helmholtz free energy (Hong et al., 2009), as:

$$\begin{aligned} \widehat{\mathrm{W}}'(\mathbf{F}_s, \mu) &= \frac{\lambda_0^{-3}}{2}NkT\left[\lambda_0^2 I' - 3 - 2\log\left(\lambda_0^3 J'\right)\right] \\ &- \frac{kT}{v}\left[\left(J' - \lambda_0^{-3}\right)\log\frac{J'}{\lambda_0^3 J' - 1}\right] - \frac{kT}{v}\frac{\chi}{\lambda_0^6 J'}, \end{aligned} \tag{113}$$

where $\mathbf{F}_s$ is the deformation gradient of the current state relative to the free-swelling state, F_{iK} is the components of $\mathbf{F}_s$, $I' = F_{iK}F_{iK}$, $J' = \det\mathbf{F}_s$, N is the number of polymeric chains per reference volume, v is the volume per solvent molecule, kT is the absolute temperature in the unit of energy, χ is a dimensionless measure of the surface energy between the network and fluid. When $\chi > 0$, the fluid molecules like themselves better than they like the long-chained polymers. We should note that the free-energy density function is the free energy density for the drained state. Physically, Eq. (113) means that the free energy contains three contributions: elastic energy of polymer chains (*i.e.*, the first term), mixing entropy (*i.e.*, the second term), and surface energy between solid skeleton and fluid (*i.e.*, the third term).

According to Eq. (96), Eq. (100) and the linearization process detailed in Section 5, we can obtain the mechanical parameters of a porous medium with macromolecular network microstructure in its drained state, *i.e.*, the drained bulk modulus:

$$K_d = \frac{kT}{v}\left[\log\left(\lambda_0^3 - 1\right) + \frac{1}{\lambda_0^3 - 1} - \frac{\chi}{\lambda_0^6}\right] + \frac{2}{3}\frac{NkT}{\lambda_0}, \tag{114}$$

and the shear modulus:

$$G = \frac{NkT}{\lambda_0}, \tag{115}$$

Using the language of poromechanics, we will rewrite Eqs. (114) and (115). Firstly, we observe that Eq. (5) reduces to NkT for $\lambda_0 = 1$, *i.e.*, the dry gel state. In other words, NkT represents the shear modulus of the solid skeleton G_s. It should be noted that $G_s = NkT$ is consistent with the shear modulus of rubber (Treloar, 1975).

Secondly, we use porosity φ in the current configuration to replace the free-swelling stretch λ_0 by $\varphi = \frac{\lambda_0^3 - 1}{\lambda_0^3}$. We should note that φ is determined by the dimensionless surface energy χ by (Hong et al., 2009):

$$Nv\left[-1 + \varphi + (1-\varphi)^{\frac{1}{3}}\right] + \log(\varphi) + 1 - \varphi + (1-\varphi)^2\chi = 0, \tag{116}$$

Given that $\varphi = \frac{\lambda_0^3 - 1}{\lambda_0^3}$ and $G_s = NkT$, the drained bulk modulus can be rewritten as

$$K_d = \frac{kT}{v}\left[\log\left(\frac{\varphi}{1-\varphi}\right) + \frac{1-\varphi}{\varphi} - \chi(1-\varphi)^2\right] + \frac{2}{3}NkT(1-\varphi)^{\frac{1}{3}}, \tag{117}$$

whereas the shear modulus can be rewritten as:

$$G = G_s(1-\varphi)^{\frac{1}{3}}. \tag{118}$$

where φ is determined by the dimensionless surface energy χ by Eq. (116).

Finally, Eqs. (111), (112), (117), and (118) give the coefficients in Eq. (110) in terms of the properties of solid skeleton, fluid and solid-fluid surface.

6.2. *Liquid inclusions*

For illustration, consider a porous medium containing liquid-filled spherical pores of radius R, as shown in Fig. 4. Assume the pores are connected by microchannels so that the liquid can move from pore to another, and the effect of these microchannels on the mechanical properties of the porous medium is negligible. The porous medium can thence be taken as a material containing liquid inclusions embedded in a solid matrix. The solid is assumed to be isotropic linear elastic, and the liquid is assumed to be linearly compressible. If the material sustains a small deformation, according to the results of Section 5, its mechanical behavior can be described using a constitutive law of the classical Biot form, *i.e.*, Eq. (110). Similar to the case of macromolecular network, we show next how to determine the coefficients in Eq. (110) by the properties of solid skeleton, fluid, and solid-fluid surface.

It should be noted that the fluid mass will not change in the undrained state, and the fluid pressure will not change in the drained state. Using the generalized self-consistent method (Christensen and Lo, 1979), we can obtain the following mechanical parameters for

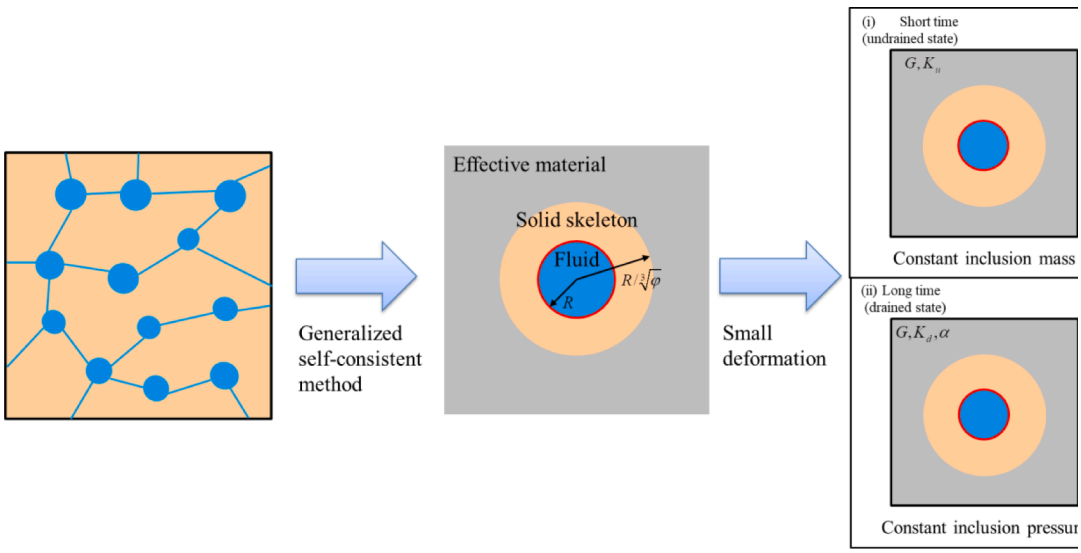

Fig. 4. Schematic of the microstructure of liquid inclusions. The liquid-filled pores are connected by microchannels so that the liquid can move from pore to another, and the effect of these microchannels on the mechanical properties of the porous medium is assumed negligible. Based upon the generalized self-consistent method (Christensen and Lo, 1979), under small deformation, we observe that there the porous medium exhibits two states: the undrained state when the volume change of the fluid is zero, and the drained state when the pore pressure is zero.

this microstructure:

Shear modulus

$$\frac{G}{G_s}=1+\frac{15\left(\frac{\gamma}{G_sR}-2\right)(-1+\nu_s)}{2(-7+5\nu_s)+\frac{\gamma}{G_sR}(-17+19\nu_s)}\varphi, \tag{119}$$

Undrained bulk modulus

$$\frac{K_u}{K_s}=\frac{2[2(-1+2\nu_s)\varphi-(1+\nu_s)]\frac{\gamma}{K_sR}+3[(1+\nu_s)+2(1-2\nu_s)\varphi]\frac{K_f}{K_s}+6(1-2\nu_s)(1-\varphi)}{2(-1+\varphi)(1+\nu_s)\frac{\gamma}{K_sR}+3(1+\nu_s)(1-\varphi)\frac{K_f}{K_s}+6(1-2\nu_s)+3(1+\nu_s)\varphi}, \tag{120}$$

Biot effective stress coefficient

$$\alpha=\frac{9(1-\nu_s)\varphi}{3[2(1-2\nu_s)+(1+\nu_s)\varphi]+2(1+\nu_s)(-1+\varphi)\varphi^{\frac{1}{3}}\frac{\gamma}{K_sR}}, \tag{121}$$

Drained bulk modulus

$$\frac{K_d}{K_s}=2\frac{3(1-2\nu_s)(1-\varphi)+[2(-1+2\nu_s)\varphi-(1+\nu_s)]\varphi^{\frac{1}{3}}\frac{\gamma}{K_sR}}{3[2(1-2\nu_s)+(1+\nu_s)\varphi]+2(1+\nu_s)(-1+\varphi)\varphi^{\frac{1}{3}}\frac{\gamma}{K_sR}}. \tag{122}$$

Here, γ is the surface energy density of the liquid-solid surface, G_s, ν_s and K_s are the shear modulus, Poisson ratio and bulk modulus of the solid, respectively, and K_f is the bulk modulus of the fluid. Note that, since the expression we obtained for the shear modulus is too complicated, only the linear form with respect to the porosity is presented in Eq. (119). Further, the methods we employed to derive these formulas belong to the scope of micromechanics, not the continuum mechanics used in this study. Therefore, considering the theoretical consistence of the present work, we leave specific details of the derivation to a separate paper devoted to the analysis of various microstructures and hence only present explicit expressions of the mechanical properties for macromolecular network and liquid inclusions here.

Note that when the solid skeleton is incompressible, Eq. (119) reduces to:

$$\frac{G}{G_s}=1+\frac{5\left(\frac{\gamma}{G_sR}-2\right)}{5\frac{\gamma}{G_sR}+6}\varphi, \tag{123}$$

which is the same as the case of dilute inclusions (Krichen et al., 2019).

6.3. Results

Using Eqs. (117) and (118), we present in Fig. 5 the predicted surface effects on the drained bulk modulus and shear modulus for a porous medium with macromolecular network microstructure. Different colors represent different shear moduli of the polymer network. We observe from Fig. 5(a) that the drained bulk modulus decreases as the surface energy is increased. Physically, this means that the greater the surface energy is, the more difficult the solid and fluid can contact with each other, and the easier to push the fluid out from the network. From Fig. 5(b) we observe that the shear modulus increases with increasing surface energy. The physical meaning is that the greater the surface energy, the smaller the porosity φ, and the denser the network.

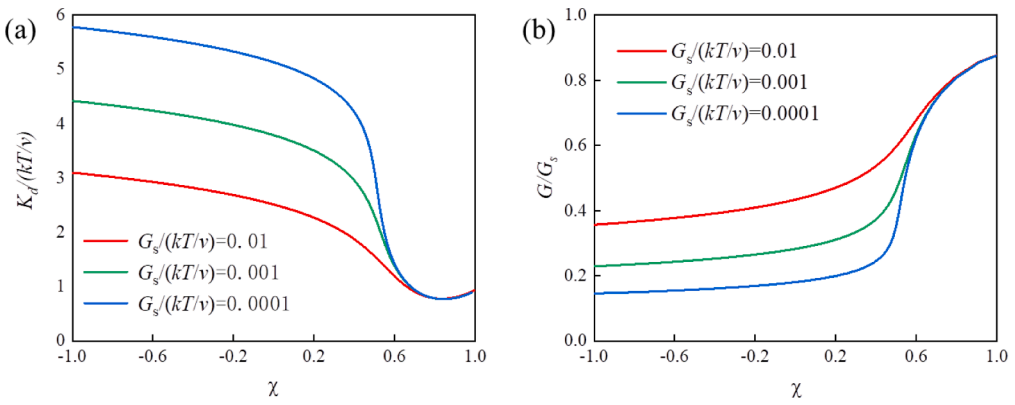

Fig. 5. Surface effects on drained bulk modulus and shear modulus for a porous medium with macromolecular network as its microstructure.χ is a dimensionless measure of the surface energy between the network and fluid. Different colors represent different shear moduli of the network.

According to Eqs. (122) and (119), we present in Fig. 6 how surface effects influence the drained bulk modulus and shear modulus of a porous medium with liquid inclusions. Different colors represent different porosities. We observe from Fig. 6(a) that the drained bulk modulus decreases with increasing surface energy. And the physical meaning is similar to that for the macromolecular network. We observe from Fig. 6(b) that the shear modulus increases as the surface energy is increased, which physically implies that part of the energy is stored on the solid-fluid surface when an external shear load is applied.

It would be interesting to compare the two microstructures. Firstly, the drained bulk modulus decreases with increasing surface energy, and the physical mechanism underlying this is the same for both cases. However, although the shear modulus increases with increasing surface energy for both cases, the physical mechanisms are different for the two cases. The surface effects influence the shear modulus by changing the swelling extent for the macromolecular network, while surface effects influence the shear modulus by storage surface energy for liquid inclusions. In fact, the surface energy of the macromolecular network only depends on its bulk deformation (see Eq. (113)), thus does not change when external shear loading is applied on the network.

Secondly, since the shear modulus increases with increasing surface energy for both cases, why do we intuitively conjecture that the existence of fluid softens the macromolecular network but stiffens the porous medium with embedded liquid inclusion (as described by the fourth paragraph of the Introduction)? In fact, we have chosen two different reference states when we make the stiffness comparison. For the macromolecular network, the reference state is the dry state. In the dry state, the polymer chains shrink together and do not want to contact with their environment. (The state of drying a bulk of hydrogel and putting it in the air approaches to this state, which is the reason why we name the state of polymer chains shrinking together as the dry state.) Actually, this state implies that the surface energy between the network and environment is infinite. For a macromolecular network, the reference state is the state of no surface effects (*i.e.*, $\gamma = 0$). In summary, when we consider how the presence of fluid may affect the stiffness of a porous medium, different reference states chosen may lead to conflict intuitions, as discussed in the introduction of this paper.

7. Discussion of surface effects

Mathematically, the constitutive relation of (94) derived for a porous medium with surface effects is similar with that obtained for a porous medium without surface effects (Coussy et al., 1998a). The question therefore is: how does the solid-fluid interface inside the porous medium affect its constitutive behaviors?

To answer the question, we explain how the surface stress balances with the stress on solid first. Consider a fluid-saturated porous medium with surface effects in a free state. In this case, the fluid inside the porous medium has the same pressure as the fluid in the outside (environment), which can be assumed to be zero for simplicity. We will therefore focus only on the mechanical state of the solid skeleton and the solid-fluid surface.

With no external load applied, the total stress is zero:

$$\mathbf{S} = 0. \tag{124}$$

For the free state, according to (23), (24), (32), (33), (63) and (79), we have:

$$S = S_s + S_{surf} + S_f, \tag{125}$$

so that

$$\begin{aligned} &\mathbf{S}(\mathbf{C}_s = 0, m = 0, T = T_0) \\ &= \mathbf{S}_s(\mathbf{C}_s = 0, m = 0, T = T_0) + \mathbf{S}_{surf}(\mathbf{C}_s = 0, m = 0, T = T_0) \\ &= 0. \end{aligned} \tag{126}$$

In general, there is surface stress on the solid-fluid interface, *i.e.* $\mathbf{S}_{surf}(\mathbf{C}_s = \mathbf{0}, m = 0, T = T_0) \neq 0$. According to (126), both the solid-

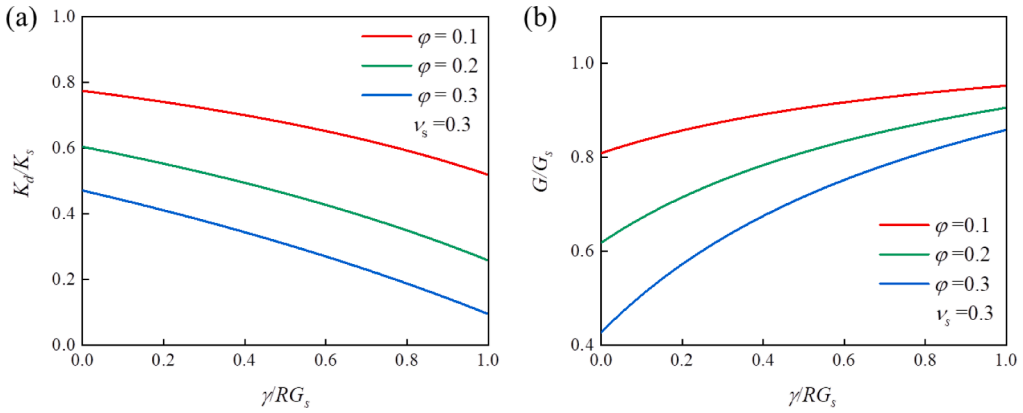

Fig. 6. The influence of surface effects on the effective mechanical properties of the porous medium containing spherical liquid inclusions. Different colors represent different porosities ($\nu_s = 0.3$).

fluid surface and the solid skeleton in the porous medium are in a state of residual stresses:

$$\mathbf{S}_{surf}(\mathbf{C}_s=\mathbf{0}, m=0, T=T_0)\neq 0, \mathbf{S}_s(\mathbf{C}_s=\mathbf{0}, m=0, T=T_0)\neq 0. \tag{127}$$

The physical meaning of (126) is that residual stress in the solid skeleton is balanced by residual stress on the solid-fluid surface. This equilibrium is similar to recent thermodynamic models, which emphasize the role of surface energy in adsorption/desorption induced swelling/shrinkage of porous materials (Li and Feng, 2016; Pan and Connell, 2007; Vandamme et al., 2010). They believed that the residual surface stress of solid-fluid interface induces residual stress in solid skeleton, which causes elastic strain in the solid skeleton even under a stress-free condition. Adsorption decreases the surface stress and consequently releases part of the elastic strain, which appears as swelling of the porous medium. These models have been used to quantitatively capture the evolution of strain and permeability during CO_2 pressurization (Li and Feng, 2016; Vandamme et al., 2010). The existence of a swelling-contraction transition point and the anisotropic swelling behavior of coal specimens have also been predicted (Espinoza et al., 2013).

Another more interesting example of swelling induced by surface effects stems from hydrogels. In the early years, a kind of special polymer was discovered. If the polymer was placed in an aqueous environment, the surface energy (or mixing enthalpy as in existing literature) between the polymer and water showed a bi-stable change with respect to temperature (Afroze et al., 2000; Schild, 1992). When this polymer is transformed to a hydrogel via a cross-linking agent, it has been found that the hydrogel exhibits snap-through instability during heating and/or cooling. Physical mechanisms underlying such snap-through instability of the temperature-sensitive hydrogel were explored by developing a large deformation theory of the hydrogel (Cai and Suo, 2011). These authors constructed first the Helmholtz free energy of the hydrogel by accounting for surface energy between the polymer network and water. Then they substituted the surface energy obtained by Afroze et al. (Afroze et al., 2000) into this free energy and found that, at a low temperature ($T = 304$ K), the free-energy function has a single minimum at a large volume, corresponding to a stable state of equilibrium - the swollen state. At a higher temperature ($T = 306$ K), the free-energy function has a single minimum at a small volume, corresponding to a stable state of equilibrium - the shrunk state. For an intermediate range of temperature, the free energy function has two local minima and one local maximum: the lower minimum corresponds to a stable state of equilibrium, the higher minimum corresponds to a metastable state of equilibrium, and the maximum corresponds to an unstable state of equilibrium.

It should be noted that although the surface effects (*i.e.*, swelling) of hydrogels have been well explained, the theoretical framework developed (Cai and Suo, 2011) falls within the classical poromechanics, with residual stress on solid-fluid surface neglected. In general, a continuum framework should contain contributions from all types of energy in the system (*i.e.*, fluid-saturated porous medium), from which equilibrium corresponding to each energy type can be derived. In fact, although Cai and Suo ignored surface stress on solid-fluid interfaces in their theoretical framework, the free energy they constructed accounts for the influence of surface effects. This is why their model can be used to explain the phenomenon related to surface effects. Such result is thought-provoking: does this mean that, when the fluid-saturated porous medium (hydrogel) deforms, it does not overcome the surface stress to do work? As discussed at the end of Section 4.3.2, the present study provides a theoretical basis for this treatment: even if surface stress is considered, the solid-fluid interfaces and solid skeleton together can be regarded as a special type of solid, thus offering convenience for using the classical framework of poromechanics to deal with porous media with surface effects.

Further, the framework developed in the present study enables the calculation of residual stress on solid-fluid interface. For illustration, we use the Helmholtz free energy Eq. (113) from existing literature (Hong et al., 2009), which has been used to analyze fluid-filled macromolecular network in Section 6, to quantify the surface stress on hydrogel. The Helmholtz free energy can be rewritten as:

$$\Psi = \Psi_s + \Psi_{surf}, \tag{128}$$

where Ψ_s is the free energy of the solid given by:

$$\Psi_s = \frac{\lambda_0^{-3}}{2} NkT\left[\lambda_0^2 I' - 3 - 2\log\left(\lambda_0^3 J'\right)\right], \tag{129}$$

and Ψ_{surf} is the free energy of solid-fluid interface given by:

$$\Psi_{surf} = -\frac{kT}{v}\left[\left(J' - \lambda_0^{-3}\right)\log\frac{J'}{\lambda_0^3 J' - 1}\right] - \frac{kT}{v}\frac{\chi}{\lambda_0^6 J'}. \tag{130}$$

The first term of Eq. (130) named mixing entropy represents the contribution of solid-fluid surface entropy, and the second term of Eq. (130) named mixing enthalpy represents the solid-fluid surface enthalpy. By the way, the entropy and enthalpy of mixing are established by Flory and Huggins (Flory, 1942; Huggins, 1941) individually, laying thus the foundations of hydrogel thermodynamics.

According Eq. (94), the second Piola-Kirchhoff stress can be obtained by

$$\mathbf{S} = \frac{\partial \Psi}{\partial \mathbf{C}_s}. \tag{131}$$

For hydrogels, the second Piola-Kirchhoff stress can thence be obtained as:

$$\frac{S_{KL}}{kT/v} = \lambda_0^{-3} N v F_{iK}^{-1}\left(\lambda_0^2 F_{iL} - H_{iL}\right) - F_{iK}^{-1}\left[-\frac{1}{\lambda_0^3} + J^{'}\log\frac{J^{'}}{\lambda_0^3 J^{'} - 1} - \frac{\chi}{\lambda_0^6 J^{'}}\right] H_{iL}, \tag{132}$$

where H_{iL} is the transpose of the inverse of deformation gradient (*i.e.*, $\mathbf{H} = \mathbf{F}_s^{-T}$). As the total stress is zero, we obtain the following balance of force:

$$F_{iK}^{-1}\left[-\frac{1}{\lambda_0^3} + J^{'}\log\frac{J^{'}}{\lambda_0^3 J^{'} - 1} - \frac{\chi}{\lambda_0^6 J^{'}}\right] H_{iL} = \lambda_0^{-3} N v F_{iK}^{-1}\left(\lambda_0^2 F_{iL} - H_{iL}\right), \tag{133}$$

where the LHS represents the surface stress on solid-fluid surface, and the RHS represents the residual stress in solid skeleton. In fact, Eq. (133) gives the expression of surface stress in hydrogel. The physical meaning of Eq. (133) is that surface stress on solid-fluid surface is balanced by residual stress in solid skeleton when the hydrogel is in free-swelling state. For a hydrogel in free state (*i.e.*, $F_{iK} = I_{iK}^{'}, H_{iL} = I_{iL}^{'}$), there exists only axial stresses, implying that surface effects will generate swelling of the gel but cause no shear deformation.

In recent years, the classical Biot theory (Biot, 1941) has been employed to describe the small deformation behaviors of fluid-saturated porous media containing micro or nanoscale pores, *e.g.*, hydrogel (Hu et al., 2010) and liver tissue (Wang et al., 2020), where surface effects play important roles. However, in the presence of surface effects, the critical issue is whether Biot theory can be generally used without losing rationality. With strict mathematical development, this study reaches an important conclusion: under small deformation, as long as the restriction in Section 4.1 for each constituent is satisfied, the mechanical behaviors of a fluid-saturated porous medium with any pore size can be described using Biot theory, regardless of surface effects. The experimental results of cytoplasmic (pore size: ~30 nm) rheology are in line with the predictions of the Biot theory (Moeendarbary et al., 2013), consistent with the theoretical results of the current study.

While our linearization results show that the mechanical behavior of a saturated porous medium with surface effects can still be described by Biot theory, the results also demonstrate the dependence of its moduli upon surface effects. This is the main difference between our theory and the existing theories of porous media with surface effects (Li and Feng, 2016). Existing studies believed that, in the presence of surface effects, the volumetric behavior needs to be modified but not the shear behavior. Nonetheless, recent results (Mancarella et al., 2016a) showed that, for a composite constructed by embedding small liquid inclusions (droplets) in a solid elastic matrix (which may be regarded as a special liquid filled porous media), surface tension does cause changes in its shear modulus. In fact, our estimations in Section 6 have proved that surface effects significantly affect both the effective shear modulus and drained bulk modulus of a fluid saturated porous medium. In follow-up studies, we will select fluid saturated porous media with representative microstructures, *e.g.*, the macromolecular network (Hong et al., 2009, 2008), small liquid inclusions embedded in soft matrix (Chen et al., 2018), and saturated cellular foam with cubic unit cells (Xia et al., 2011), to systematically quantify the influence of surface effects on key poroelastic coefficients. We will further investigate how surface effects influence the other two properties, *i.e.*, the bulk modulus K_u in undrained state and the Biot effective stress coefficient α. For example, we will show how surface effects on undrained bulk modulus depend on the ratio between the bulk modulus of the fluid and that of the solid skeleton. Further, the technical details omitted in this study will be presented in these follow-up studies.

8. Concluding remarks

A theoretical framework has been developed on the basis of mixture theory to characterize the mechanical behaviors of porous media with surface effects and check the validity of classical poromechanics theory (*e.g.*, Biot theory) at sufficiently small scales where surface effects play important roles. Main results are summarized below.

(1) Based on the homogenization assumption in mixture theory and Cauchy's theorem, we prove that, mathematically, surface stress on solid-fluid interface can be expressed by a second order tensor defined at each point of the porous medium.
(2) The developed framework includes mass conservation momentum balance as well as first and second laws of thermodynamics.
(3) Based on the Clausius–Duhem inequality, restrictions on constitutive laws of porous material under surface effects are discussed.
(4) We linearize the developed constitutive laws and prove that, in the presence of surface effects, the classical Biot theory still holds (at least in format) under small deformation; however, relevant parameters (*e.g.*, effective moduli) appearing in the constitutive laws are dependent upon surface effects, thus need to be determined separately from either experimental measurements or theoretical modeling once the microstructure of the fluid-saturated porous medium is known a priori.
(5) The microstructures of a macromolecular network and an elastic matrix embedded with liquid inclusions have been separately employed as prototypes to demonstrate how their mechanical behaviors are related to the properties of three constituents, *i.e.*, solid, fluid and solid-fluid interface, and determine explicitly the parameters appearing in their constitutive relations.

The theoretical framework developed in the present study lays a solid foundation for further theoretical and experimental studies of porous media with surface effects.

Declaration of Competing Interest

The authors declare that they have no known competing financial interests or personal relationships that could have appeared to influence the work reported in this paper.

Acknowledgements

This work was supported by the National Natural Science Foundation of China (11972185), and the Open Fund of the State Key Laboratory of Mechanics and Control of Mechanical Structures (MCMS-I-0219K01 and MCMS-E-0219K02).

References

Abousleiman, Y., Cui, L., 1998. Poroelastic solutions in transversely isotropic media for wellbore and cylinder. Int. J. Solids Struct. 35, 4905–4929.
Afroze, F., Nies, E., Berghmans, H., 2000. Phase transitions in the system poly (N-isopropylacrylamide)/water and swelling behavior of the corresponding networks. J. Mol. Struct. 554, 55–68.
Anand, L., 2017. A large deformation poroplasticity theory for microporous polymeric materials. J. Mech. Phys. Solids 98, 126–155.
Aouaini, F., Knani, S., Yahia, M.B., Lamine, A.B., 2015. Statistical physics studies of multilayer adsorption isotherm in food materials and pore size distribution. Physica A 432, 373–390.
Armero, F., 1999. Formulation and finite element implementation of a multiplicative model of coupled poro-plasticity at finite strains under fully saturated conditions. Comput. Method. Appl. M. 171, 205–241.
Avramidis, S., Englezos, P., Papathanasiou, T., 1992. Dynamic nonisothermal transport in hygroscopic porous media: moisture diffusion in wood. AIChE J. 38, 1279–1287.
Baer, M., Nunziato, J., 1986. A two-phase mixture theory for the deflagration-to-detonation transition (DDT) in reactive granular materials. Int. J. Multiphase Flow 12, 861–889.
Bennethum, L.S., Murad, M.A., Cushman, J.H., 2000. Macroscale thermodynamics and the chemical potential for swelling porous media. Transport Porous Med. 39, 187–225.
Biot, M.A., 1941. General theory of three dimensional consolidation. J. Appl. Phys. 12, 155–164.
Biot, M.A., 1977. Variational Lagrangian-thermodynamics of nonisothermal finite strain mechanics of porous solids and thermomolecular diffusion. Int. J. Solids Struct. 13, 579–597.
Biot, M.A., Temple, G., 1972. Theory of finite deformations of porous solids. Indiana U. Math. J. 21, 597–620.
Biot, M.A., Willis, D., 1957. The elastic coeffcients of the theory of consolidation. J. Appl. Mech. 24, 594–601.
Bowen, R.M., 1980. Incompressible porous media models by use of the theory of mixtures. Int. J. Eng. Sci. 18, 1129–1148.
Cai, S., Suo, Z., 2011. Mechanics and chemical thermodynamics of phase transition in temperature-sensitive hydrogels. J. Mech. Phys. Solids 59, 2259–2278.
Chen, X., Li, M., Yang, M., Liu, S., Genin, G.M., Xu, F., Lu, T.J., 2018. The elastic fields of a compressible liquid inclusion. Extreme Mech. Lett. 22, 122–130.
Cheng, A.H.-D., 2016. Poroelasticity. Springer.
Christensen, R.M., Lo, K.H., 1979. Solutions for effective shear properties in three phase sphere and cylinder models. J. Mech. Phys. Solids 27, 315–330.
Clarkson, C.R., Solano, N., Bustin, R.M., Bustin, A., Chalmers, G., He, L., Melnichenko, Y.B., Radliński, A., Blach, T.P., 2013. Pore structure characterization of North American shale gas reservoirs using USANS/SANS, gas adsorption, and mercury intrusion. Fuel 103, 606–616.
Coussy, O., Dormieux, L., Detournay, E., 1998a. From mixture theory to Biot's approach for porous media. Int. J. Solids Struct. 35, 4619–4635.
Coussy, O., 1989. Thermomechanics of saturated porous solids in finite deformation. Eur. J. Mech. A/Solids 8, 1–14.
Coussy, O., 2004. Poromechanics. John Wiley & Sons, Ltd., Chichester.
Coussy, O., 2007. Revisiting the constitutive equations of unsaturated porous solids using a Lagrangian saturation concept. Int. J. Numer. Anal. Met. 31, 1675–1694.
Coussy, O., 2011. Mechanics and Physics of Porous Solids. John Wiley & Sons.
Coussy, O., Eymard, R., Lassabatere, T., 1998b. Constitutive modeling of unsaturated drying deformable materials. J. Eng. Mech. 124, 658–667.
Cowin, S.C., 1999. Bone poroelasticity. J. Biomech. 32, 217–238.
Cuenot, S., Frétigny, C., Demoustier-Champagne, S., Nysten, B., 2004. Surface tension effect on the mechanical properties of nanomaterials measured by atomic force microscopy. Phys. Rev. B 69, 165410.
Cui, X., Bustin, R.M., 2005. Volumetric strain associated with methane desorption and its impact on coalbed gas production from deep coal seams. AAPG Bull. 89, 1181–1202.
Darcy, H., 1856. Les Fontaines Publiques De La Ville De Dijon (The Public Fountains of the City of Dijon). Dalmont, Paris.
de Boer, R., 1996. Highlights in the historical development of the porous media theory: toward a consistent macroscopic theory. Appl. Mech. Rev. 49, 201–262.
de Boer, R., Ehlers, W., 1986a. On the problem of fluid-and gas-filled elasto-plastic solids. Int. J. Solids Struct. 22, 1231–1242.
de Boer, R., Ehlers, W., 1986b. Theorie der Mehrkomponentenkontinua mit Anwendung auf Bodenmechanische Probleme, Teil I, Forschungsberichte aus dem Fachbereich Bauwesen. Heft 40. Essen: Universität-GH-Essen.
de Boer, R., Kowalski, S.J., 1983. A plasticity theory for fluid-saturated porous solids. Int. J. Eng. Sci. 21, 1343–1357.
de Boer, R., Lade, P., 10-Bauwesen, E.U.F., 1991. Towards a General Plasticity Theory For Empty and Saturated Porous solids. Forschungsbericht aus Dem Fachbereich Bauwesen. Universität Essen.
Detournay, E., Cheng, A.H.-D., 1993. Fundamentals of poroelasticity. In: Hudson, J.A. (Ed.), Comprehensive Rock Engineering: Principles, Practices and Projects, vol. 2. Pergamon Press, Oxford, UK, pp. 113–171.
Dhanarajan, A.P., Misra, G.P., Siegel, R.A., 2002. Autonomous chemomechanical oscillations in a hydrogel/enzyme system driven by glucose. J. Phys. Chem. A 106, 8835–8838.
Diebels, S., Ehlers, W., 1996. Dynamic analysis of a fully saturated porous medium accounting for geometrical and material non-linearities. Int. J. Numer. Meth. Eng. 39, 81–97.
Duan, H.L., Wang, J., Huang, Z.P., Karihaloo, B.L., 2005a. Eshelby formalism for nano-inhomogeneities. Proc. R. Soc. A 461, 3335–3353.
Duan, H.L., Wang, J., Huang, Z.P., Karihaloo, B.L., 2005b. Size-dependent effective elastic constants of solids containing nano-inhomogeneities with interface stress. J. Mech. Phys. Solids 53, 1574–1596.
Ducloué, L., Pitois, O., Goyon, J., Chateau, X., Ovarlez, G., 2014. Coupling of elasticity to capillarity in soft aerated materials. Soft Matter. 10, 5093–5098.
Ehlers, W., 2009. Challenges of porous media models in geo-and biomechanical engineering including electro-chemically active polymers and gels. Int. J. Adv. Eng. Sci. Appl. Math. 1, 1–24.
Espinoza, D., Vandamme, M., Dangla, P., Pereira, J.M., Vidal-Gilbert, S., 2013. A transverse isotropic model for microporous solids: application to coal matrix adsorption and swelling. J. Geophys. Res-Sol. Ea. 118, 6113–6123.
Espinoza, D.N., Vandamme, M., Pereira, J.-.M., Dangla, P., Vidal-Gilbert, S., 2014. Measurement and modeling of adsorptive-poromechanical properties of bituminous coal cores exposed to CO_2: adsorption, swelling strains, swelling stresses and impact on fracture permeability. Int. J. Coal Geol. 134, 80–95.
Flory, P.J., 1942. Thermodynamics of high polymer solutions. J. Chem. Phys. 10, 51–61.
Gajo, A., 2010. A general approach to isothermal hyperelastic modelling of saturated porous media at finite strains with compressible solid constituents. Proc. R. Soc. A 466, 3061–3087.

Guenther, M., Gerlach, G., Corten, C., Kuckling, D., Muller, M., Shi, Z., Sorber, J., Arndt, K.F., 2007. Application of polyelectrolytic temperature-responsive hydrogels in chemical sensors. Macromol. Symp. 254, 314–321.
Gurtin, M.E., Murdoch, A.I., 1975. A continuum theory of elastic material surfaces. Arch. Ration. Mech. An. 57, 291–323.
Hicsasmaz, Z., Clayton, J., 1992. Characterization of the pore structure of starch based food materials. Food Struct. 11, 115–132.
Holzapfel, G.A., 2002. Nonlinear solid mechanics: a continuum approach for engineering science. Meccanica 37, 489–490.
Hong, W., Liu, Z., Suo, Z., 2009. Inhomogeneous swelling of a gel in equilibrium with a solvent and mechanical load. Int. J. Solids Struct. 46, 3282–3289.
Hong, W., Zhao, X., Zhou, J., Suo, Z., 2008. A theory of coupled diffusion and large deformation in polymeric gels. J. Mech. Phys. Solids 56, 1779–1793.
Howse, J.R., Topham, P., Crook, C.J., Gleeson, A.J., Bras, W., Jones, R.A., Ryan, A.J., 2006. Reciprocating power generation in a chemically driven synthetic muscle. Nano Lett 6, 73–77.
Hu, Y., Zhao, X., Vlassak, J.J., Suo, Z., 2010. Using indentation to characterize the poroelasticity of gels. Appl. Phys. Lett. 96, 121904.
Huggins, M.L., 1941. Solutions of long chain compounds. J. Chem. Phys. 9, 440. -440.
Jing, G., Duan, H.L., Sun, X., Zhang, Z., Xu, J., Li, Y., Wang, J., Yu, D., 2006. Surface effects on elastic properties of silver nanowires: contact atomic-force microscopy. Phys. Rev. B 73, 235409.
Kou, S.C., Poon, C.S., Etxeberria, M., 2014. Residue strength, water absorption and pore size distributions of recycled aggregate concrete after exposure to elevated temperatures. Cement Concrete Compos. 53, 73–82.
Krichen, S., Liu, L., Sharma, P., 2019. Liquid inclusions in soft materials: capillary effect, mechanical stiffening and enhanced electromechanical response. J. Mech. Phys. Solids 127, 332–357.
Le Couteur, D.G., Fraser, R., Kilmer, S., Rivory, L.P., McLean, A.J., 2005. The hepatic sinusoid in aging and cirrhosis. Clin. Pharmacokinet. 44, 187–200.
Leclaire, P., Cohen-Ténoudji, F., Aguirre-Puente, J., 1994. Extension of Biot's theory of wave propagation to frozen porous media. J. Acoust. Soc. Am. 96, 3753–3768.
Leij, F.J., Ghezzehei, T.A., Or, D., 2002. Modeling the dynamics of the soil pore-size distribution. Soil Till. Res. 64, 61–78.
Li, C., Feng, J., 2016. Adsorption-induced permeability change of porous material: a micromechanical model and its applications. Arch. Appl. Mech. 86, 465–481.
Mancarella, F., Style, R.W., Wettlaufer, J.S., 2016a. Interfacial tension and a three-phase generalized self-consistent theory of non-dilute soft composite solids. Soft Matter. 12, 2744–2750.
Mancarella, F., Style, R.W., Wettlaufer, J.S., 2016b. Surface tension and the Mori-Tanaka theory of non-dilute soft composite solids. Proc. R. Soc. A 472, 20150853.
Marsden, J.E., Hughes, T.J.R., 1994. Mathematical Foundations of Elasticity. Dover Civil and Mechanical Engineering. Dover Publications.
Miller, R.E., Shenoy, V.B., 2000. Size-dependent elastic properties of nanosized structural elements. Nanotechnology 11, 139.
Moeendarbary, E., Valon, L., Fritzsche, M., Harris, A.R., Moulding, D.A., Thrasher, A.J., Stride, E., Mahadevan, L., Charras, G.T., 2013. The cytoplasm of living cells behaves as a poroelastic material. Nat. Mater. 12, 253–261.
Mow, V.C., Holmes, M.H., Lai, W.M., 1984. Fluid transport and mechanical properties of articular cartilage: a review. J. Biomech. 17, 377–394.
Nedjar, B., 2013. Formulation of a nonlinear porosity law for fully saturated porous media at finite strains. J. Mech. Phys. Solids 61, 537–556.
Nur, A., Byerlee, J.D., 1971. An exact effective stress law for elastic deformation of rock with fluids. J. Geophys. Res. 76, 6414–6419.
Oikonomopoulou, V.P., Krokida, M.K., Karathanos, V.T., 2011. Structural properties of freeze-dried rice. J. Food Eng. 107, 326–333.
Pan, Z., Connell, L.D., 2007. A theoretical model for gas adsorption-induced coal swelling. Int. J. Coal Geol. 69, 243–252.
Radlinski, A., Mastalerz, M., Hinde, A., Hainbuchner, M., Rauch, H., Baron, M., Lin, J., Fan, L., Thiyagarajan, P., 2004. Application of SAXS and SANS in evaluation of porosity, pore size distribution and surface area of coal. Int. J. Coal Geol. 59, 245–271.
Rice, J.R., Cleary, M.P., 1976. Some basic stress diffusion solutions for fluid-saturated elastic porous media with compressible constituents. Rev. Geophys. 14, 227–241.
Schild, H.G., 1992. Poly (N-isopropylacrylamide): experiment, theory and application. Prog. Polym. Sci. 17, 163–249.
Schrefler, B., Simoni, L., Turska, E., Zhan, X., 1993. Zur berechnung von ungesättigten konsolidationsproblemen. Bauingenieur-Germany 68, 375–384.
Shuttleworth, R., 1950. The surface tension of solids. Proc. Phys. Soc. A 63, 444–457.
Style, R.W., Boltyanskiy, R., Allen, B., Jensen, K.E., Foote, H.P., Wettlaufer, John S., Dufresne, E.R., 2014. Stiffening solids with liquid inclusions. Nat. Phys. 11, 82–87.
Style, R.W., Wettlaufer, J.S., Dufresne, E.R., 2015. Surface tension and the mechanics of liquid inclusions in compliant solids. Soft Matter. 11, 672–679.
Suzuki, A., Yoshikawa, S., Bai, G., 1999. Shrinking pattern and phase transition velocity of poly (N-isopropylacrylamide) gel. J. Chem. Phys. 111, 360–367.
Treloar, L.R.G., 1975. The Physics of Rubber Elasticity. 3rd Clarendon Press, Oxford.
Vandamme, M., Brochard, L., Lecampion, B., Coussy, O., 2010. Adsorption and strain: the CO_2-induced swelling of coal. J. Mech. Phys. Solids 58, 1489–1505.
Vennat, E., Denis, M., David, B., Attal, J.-P., 2015. A natural biomimetic porous medium mimicking hypomineralized enamel. Dent. Mater. 31, 225–234.
Vidyasagar, A., Majewski, J., Toomey, R., 2008. Temperature induced volume-phase transitions in surface-tethered poly (N-isopropylacrylamide) networks. Macromolecules 41, 919–924.
Vogel, H.-J., Roth, K., 2001. Quantitative morphology and network representation of soil pore structure. Adv. Water Resour. 24, 233–242.
von Terzaghi, K., 1923. Die Berechnug der Durchlassigkeit des Tones aus dem Verlauf der hydromechanischen Spannungserscheinungen. Sitzungsber. Akad. Wiss. Wien Math.-Naturwiss. 132, 125–138.
Wahlsten, A., Pensalfini, M., Stracuzzi, A., Restivo, G., Hopf, R., Mazza, E., 2019. On the compressibility and poroelasticity of human and murine skin. Biomech. Model. Mechan. 18, 1079–1093.
Wang, M., Liu, S., Xu, Z., Qu, K., Li, M., Chen, X., Xue, Q., Genin, G.M., Lu, T.J., Xu, F., 2020. Characterizing poroelasticity of biological tissues by spherical indentation: an improved theory for large relaxation. J. Mech. Phys. Solids 138, 103920.
Wei, F., Lan, F., Liu, B., Liu, L., Li, G., 2016. Poroelasticity of cell nuclei revealed through atomic force microscopy characterization. Appl. Phys. Lett. 109, 213701.
Weinstein, T., Bennethum, L.S., 2006. On the derivation of the transport equation for swelling porous materials with finite deformation. Int. J. Eng. Sci. 44, 1408–1422.
White, F.M., 2010. Fluid Mechanics. McGraw-Hill, New York.
Williams, J.L., 1992. Ultrasonic wave propagation in cancellous and cortical bone: prediction of some experimental results by Biot's theory. J. Acoust. Soc. Am. 91, 1106–1112.
Xia, R., Feng, X.-Q., Wang, G.-F., 2011. Effective elastic properties of nanoporous materials with hierarchical structure. Acta Mater. 59, 6801–6808.
Yang, J., Di, Q., Zhao, J., Wang, L., 2010. Fractal dimension of pore size distribution inside matrix of plant materials and drying behavior. In: Proceedings of the 14th International Heat Transfer Conference, pp. 91–99.
Zhang, Y., 2018. Mechanics of adsorption-deformation coupling in porous media. J. Mech. Phys. Solids 114, 31–54.